Search for the neutral Higgs bosons of the Minimal Supersymmetric Standard Model in pp collisions at sqrt(s)=7 TeV with the ATLAS detector

Published for SISSA by Springer

Received: November 29, 2012
Accepted: January 27, 2013
Published: February 15, 2013

Search for the neutral Higgs bosons of the minimal supersymmetric standard model in pp collisions at $\sqrt{s} = 7\,\text{TeV}$ with the ATLAS detector

The ATLAS collaboration

E-mail: atlas.publications@cern.ch

Abstract: A search for neutral Higgs bosons of the Minimal Supersymmetric Standard Model (MSSM) is reported. The analysis is based on a sample of proton-proton collisions at a centre-of-mass energy of 7 TeV recorded with the ATLAS detector at the Large Hadron Collider. The data were recorded in 2011 and correspond to an integrated luminosity of $4.7\,\text{fb}^{-1}$ to $4.8\,\text{fb}^{-1}$. Higgs boson decays into oppositely-charged muon or τ lepton pairs are considered for final states requiring either the presence or absence of b-jets. No statistically significant excess over the expected background is observed and exclusion limits at the 95% confidence level are derived. The exclusion limits are for the production cross-section of a generic neutral Higgs boson, ϕ, as a function of the Higgs boson mass and for $h/A/H$ production in the MSSM as a function of the parameters m_A and $\tan\beta$ in the m_h^{max} scenario for m_A in the range of 90 GeV to 500 GeV.

Keywords: Hadron-Hadron Scattering

doi:10.1007/JHEP02(2013)095

JHEP02(2013)095

Contents

JHEP02(2013)095

1 Introduction

Discovering the mechanism responsible for electroweak symmetry breaking is one of the major goals of the physics programme at the Large Hadron Collider (LHC) [1]. In the Standard Model this mechanism requires the existence of a single scalar particle, the Higgs boson [2–6]. The recent discovery of a particle compatible with the Higgs boson at the LHC [7, 8] provides further evidence in support of this simple picture. Even if this recently discovered particle is shown to have properties very close to the Standard Model Higgs boson, there are still a number of problems that are not addressed. For instance, quantum corrections to the mass of the Higgs boson contain quadratic divergences. This problem can be solved by introducing supersymmetry, a symmetry between fermions and bosons, by which the divergent corrections to the Higgs boson mass are cancelled.

In the Minimal Supersymmetric Standard Model (MSSM) [9, 10], two Higgs doublets are necessary, coupling separately to up-type and down-type fermions. This results in five

physical Higgs bosons, two of which are neutral and CP-even (h, H),[1] one of which is neutral and CP-odd (A), and two of which are charged ($H^{\pm}$). At tree level their properties can be described in terms of two parameters, typically chosen to be the mass of the CP-odd Higgs boson, m_A, and the ratio of the vacuum expectation values of the two Higgs doublets, $\tan\beta$. In the MSSM, the Higgs boson couplings to τ leptons and b-quarks are strongly enhanced for a large part of the parameter space. This is especially true for large values of $\tan\beta$, in which case the decay of a Higgs boson to a pair of τ leptons or b-quarks and its production in association with b-quarks play a much more important role than in the Standard Model.

The results presented in this paper are interpreted in the context of the $m_h^{\max}$ benchmark scenario [11]. In the $m_h^{\max}$ scenario the parameters of the model are chosen such that the mass of the lightest CP-even Higgs boson, h, is maximised for a given point in the m_A–$\tan\beta$ plane, under certain assumptions. This guarantees conservative exclusion bounds from the LEP experiments. The sign of the Higgs sector bilinear coupling, μ, is generally not constrained, but for the analysis presented in this paper $\mu > 0$ is chosen as this is favoured by the measurements of the anomalous magnetic dipole moment of the muon [12].

The masses of the Higgs bosons in this scenario are such that for large values of $\tan\beta$ two of the three neutral Higgs bosons are closely degenerate in mass: for $m_A \lesssim 130\,\text{GeV}$, $m_h \simeq m_A$ and $m_H \simeq 130\,\text{GeV}$, whereas for $m_A \gtrsim 130\,\text{GeV}$, $m_H \simeq m_A$ and $m_h \simeq 130\,\text{GeV}$.

The most common MSSM neutral Higgs boson production mechanisms at a hadron collider are the b-quark associated production and gluon-fusion processes, the latter process proceeding primarily through a b-quark loop for intermediate and high $\tan\beta$. Both processes have cross-sections that increase with $\tan\beta$, with the b-associated production process becoming dominant at high $\tan\beta$ values. The most common decay modes at high $\tan\beta$ are to a pair of b-quarks or τ leptons, with branching ratios close to 90% and 10%, respectively, across the mass range considered. The direct decay into two muons occurs rarely, with a branching ratio around 0.04%, but offers a clean signature.

Previous searches for neutral MSSM Higgs bosons have been performed at LEP [13], the Tevatron [14–19] and the LHC [7, 8]. The recently observed Higgs-boson-like particle at the LHC [20, 21] is consistent with both the Standard Model and the lightest CP-even MSSM Higgs boson [22, 23]. In this paper a search for neutral MSSM Higgs bosons using $4.7\,\text{fb}^{-1}$ to $4.8\,\text{fb}^{-1}$ of proton-proton collision data collected with the ATLAS detector [24] in 2011 at the centre-of-mass energy of 7 TeV is presented. The $\mu^+\mu^-$ and $\tau^+\tau^-$ decay modes are considered, with the latter divided into separate search channels according to the subsequent τ lepton decay modes. Events from each channel are further classified according to the presence or the absence of an identified b-jet.

2 The ATLAS detector

The ATLAS experiment at the LHC is a multi-purpose particle detector with a forward-backward symmetric cylindrical geometry and nearly 4π coverage in solid angle [24]. It

[1] By convention the lighter CP-even Higgs boson is called h, the heavier CP-even Higgs boson is called H.

JHEP02(2013)095

consists of an inner tracking detector surrounded by a thin superconducting solenoid providing a 2 T axial magnetic field, electromagnetic and hadronic calorimeters, and a muon spectrometer. The inner tracking detector covers the pseudorapidity range $|\eta| < 2.5$.[2] It consists of silicon pixel, semi-conductor micro-strip, and transition radiation tracking detectors. Lead/liquid-argon (LAr) sampling calorimeters provide electromagnetic (EM) energy measurements with high granularity. A hadronic (iron/scintillator-tile) calorimeter covers the central pseudorapidity range ($|\eta| < 1.7$). The end-cap and forward regions are instrumented with LAr calorimeters for both EM and hadronic energy measurements up to $|\eta| = 4.9$. The muon spectrometer surrounds the calorimeters and incorporates three large air-core toroid superconducting magnets with bending power between 2.0 Tm and 7.5 Tm, a system of precision tracking chambers and fast detectors for triggering. A three-level trigger system is used to select events. The first-level trigger is implemented in hardware and uses a subset of the detector information to reduce the rate to at most 75 kHz. This is followed by two software-based trigger levels that together reduce the event rate to approximately 300 Hz. The trigger requirements were adjusted to changing data-taking conditions during 2011.

3 Data and Monte Carlo simulation samples

The data used in this search were recorded by the ATLAS experiment during the 2011 LHC run with proton-proton collisions at a centre-of-mass energy of 7 TeV. They correspond to an integrated luminosity of 4.7 fb^{-1} ($\tau^+\tau^-$ channels) or 4.8 fb^{-1} ($\mu^+\mu^-$ channel) after imposing the data quality selection criteria to require that all relevant detector sub-systems used in these analyses were operational.

Higgs boson production: the Higgs boson production mechanisms considered are gluon-fusion and b-associated production. The cross-sections for the first process have been calculated using HIGLU [25] and ggh@nnlo [26]. For b-associated production, a matching scheme described in reference [27] is used to combine four-flavour [28, 29] calculations and the five-flavour bbh@nlo [30] calculation. The masses, couplings and branching ratios of the Higgs bosons are computed with FeynHiggs [31]. Details of the calculations and the associated uncertainties due to the choice of the value of the strong coupling constant, the parton distribution function and the factorisation and renormalisation scales can be found in reference [32]. Gluon-fusion production is simulated with POWHEG [33], while b-quark associated production is simulated with SHERPA [34].

The $h/A/H \to \mu^+\mu^-$ and $h/A/H \to \tau^+\tau^-$ modes are considered for the decay of the Higgs boson. The A boson samples are generated for both production mechanisms and are also employed for modelling H and h production. The differences between CP-even and CP-odd eigenstates are negligible for this analysis. The signal modelling for a given combination of m_A and $\tan\beta$ takes into account all three Higgs bosons h, H and A, by

[2] ATLAS uses a right-handed coordinate system with its origin at the nominal interaction point (IP) in the centre of the detector and the z-axis along the beam pipe. The x-axis points from the IP to the centre of the LHC ring, and the y-axis points upwards. Cylindrical coordinates (r, ϕ) are used in the transverse plane, ϕ being the azimuthal angle around the beam pipe. The pseudorapidity is defined in terms of the polar angle θ as $\eta = -\ln\tan(\theta/2)$.

JHEP02(2013)095

adding the A boson mass samples corresponding to m_h, m_H and m_A according to their production cross-sections and masses in the m_h^{max}, $\mu > 0$ MSSM benchmark scenario.

For the $\tau^+\tau^-$ decay mode, 15 Monte Carlo samples are generated with Higgs boson masses in the range of 90 GeV to 500 GeV and $\tan\beta = 20$. These are scaled to the appropriate cross-sections for other $\tan\beta$ values. The simulated signal samples with m_A closest to the computed mass of H and h are used for the H and h bosons. The increase in the Higgs boson natural width with $\tan\beta$, of the order of 1 GeV in the range considered, is negligible compared to the experimental mass resolution in this channel, which is always above 10 GeV.

For the $\mu^+\mu^-$ decay mode, seven samples are generated with Higgs boson masses in the range of 110 GeV to 300 GeV and $\tan\beta = 40$. Additionally, to study the $\tan\beta$ dependence of the width of the resonance, signal samples are generated for both production modes for $m_A = 150$ GeV and 250 GeV, each at $\tan\beta = 20$ and $\tan\beta = 60$. Since the mass resolution is better in this channel, signal distributions are obtained using an interpolation procedure for different intermediate m_A–$\tan\beta$ values, as described in section 5.

The generated Monte Carlo samples for the $h/A/H \to \tau^+\tau^-$ decay modes are passed through the full GEANT4 [35, 36] detector simulation, while the samples for the $h/A/H \to \mu^+\mu^-$ decay mode are passed through the full GEANT4 detector simulation or the "fast" simulation, ATLFAST-II [35], of the ATLAS detector.

Background processes: the production of W and Z/γ^* bosons in association with jets is simulated using the ALPGEN [37] and PYTHIA [38] generators. PYTHIA is also used for the simulation of $b\bar{b}$ production, but through an interface, which ensures that the simulation is in agreement with b-quark production data [39, 40]. The $t\bar{t}$ production process is generated with MC@NLO [41] and POWHEG [42, 43]. MC@NLO is used for the generation of electroweak diboson (WW, WZ, ZZ) samples. Single-top production through the s- and t-channels, and in association with W bosons, is generated using AcerMC [44]. For all event samples described above, parton showers and hadronisation are simulated with HERWIG [45] and the activity of the underlying event with JIMMY [46]. The loop-induced $gg \to WW$ processes are generated using gg2WW [47]. The following parton distribution function sets are used: CT10 [48] for MC@NLO, CTEQ6L1 [49] for ALPGEN and modified leading-order MRST2007 [50] for PYTHIA samples.

Decays of τ leptons are simulated using either SHERPA or TAUOLA [51]. Initial-state and final-state radiation of photons is simulated using either PHOTOS [52] or, for the samples generated with SHERPA, PHOTONS++, which is a part of SHERPA. The $Z/\gamma^* \to \tau^+\tau^-$ background processes are modelled with a τ-embedded $Z/\gamma^* \to \mu^+\mu^-$ data sample described in section 6. All generated Monte Carlo background samples are passed through the full GEANT4 simulation of the ATLAS detector.

The signal and background samples are reconstructed with the same software as used for data. To take into account the presence of multiple interactions occurring in the same and neighbouring bunch crossings (referred to as pile-up), simulated minimum bias events are added to the hard process in each generated event. Prior to the analysis, simulated events are re-weighted in order to match the distribution of the number of pile-up interactions per bunch crossing in the data.

JHEP02(2013)095

4 Physics object reconstruction

An electron candidate is formed from energy deposits in the electromagnetic calorimeter associated with a charged particle track measured in the inner detector. Electrons are selected if they have a transverse energy $E_{\mathrm{T}} > 15\,\mathrm{GeV}$, lie within $|\eta| < 2.47$, but outside the transition region between the barrel and end-cap calorimeters ($1.37 < |\eta| < 1.52$), and meet quality requirements based on the expected shower shape [53].

A muon candidate is formed from a high-quality track measured in the inner detector matched to hits in the muon spectrometer [54]. Muons are required to have a transverse momentum $p_{\mathrm{T}} > 10\,\mathrm{GeV}$ and to lie within $|\eta| < 2.5$. In addition, the point of closest approach of the inner detector track must be no further than 1 cm from the primary vertex,[3] as measured along the z-axis. This requirement reduces the contamination due to cosmic-ray muons and beam-induced backgrounds.

Identified electrons and muons are isolated if there is little additional activity in the inner detector and the calorimeter around the electron or muon. The scalar sum of the transverse momenta of all tracks from the same vertex as the lepton, with p_{T} above 1 GeV and located within a cone with radius parameter[4] $\Delta R = 0.4$ around the lepton direction, must be less than 6% of the lepton momentum for the $\tau^+\tau^-$ channels, or less than 10% for the $\mu^+\mu^-$ channels. The sum excludes the track associated to the lepton itself. In addition, for the $\tau^+\tau^-$ channel, the remaining calorimetric energy within a cone of radius parameter $\Delta R = 0.2$ around the lepton direction must be less than 8% (4%) of the electron transverse energy (muon transverse momentum). The remaining energy excludes that associated to the lepton itself and an average correction due to pile-up is made.

Reconstructed electrons and muons are used to identify the leptonic decays of τ leptons (τ_{lep}). The decay of a τ lepton into an electron (muon) and neutrinos is denoted by τ_e (τ_μ).

Jets are reconstructed using the anti-k_t algorithm [55] with a radius parameter $R = 0.4$, taking three-dimensional noise-suppressed clusters of calorimeter-cell energy deposits [56] as input. The jet energy is calibrated using a combination of test-beam results, simulation and in situ measurements [57]. Jets must satisfy $E_T > 20\,\mathrm{GeV}$ and $|\eta| < 4.5$. Rare events containing a jet with associated out-of-time activity or calorimeter noise are discarded. Tracks are classified as associated tracks if they lie within $\Delta R < 0.4$ of the jet axis. To reduce the pile-up effect, the scalar sum of the transverse momenta of the associated tracks matched to the primary vertex must be at least 75% of the jet transverse momentum measured in the calorimeter. A multivariate algorithm based on a neural network is used in this analysis to tag jets, reconstructed within $|\eta| < 2.5$, that are associated with the hadronisation of b-quarks. The neural network makes use of the impact parameter of associated tracks and the reconstruction of b- and c-hadron decay vertices inside the jet [58]. The b-jet identification has an efficiency of about 70% in $t\bar{t}$ events, unless otherwise stated. The corresponding rejection factors are about 5 for jets containing charm hadrons and about 130 for light-quark or gluon jets.

[3] The primary vertex is defined as the vertex with the largest Σp_{T}^2 of the associated tracks.

[4] $\Delta R = \sqrt{(\Delta\eta)^2 + (\Delta\phi)^2}$, where $\Delta\eta$ is the difference in pseudorapidity of the two objects in question and $\Delta\phi$ is the difference between their azimuthal angles.

JHEP02(2013)095

Hadronic decays of τ leptons (τ_{had}) are characterised by the presence of one, three, or in rare cases, five charged hadrons accompanied by a neutrino and possibly neutral hadrons, resulting in a collimated shower profile in the calorimeters with only a few nearby tracks. The visible τ decay products are reconstructed in the same way as jets, but are calibrated separately to account for the different calorimeter response compared to jets. Information on the collimation, isolation, and shower profile is combined into a boosted-decision-tree discriminant to reject backgrounds from jets [59]. In this analysis, three selections are used —"loose", "medium" and "tight"— with identification efficiency of about 60%, 45% and 35%, respectively. The rejection factor against jets varies from about 20 for the loose selection to about 300 for the tight selection. A τ_{had} candidate must lie within $|\eta| < 2.5$, have a transverse momentum greater than 20 GeV, one or three associated tracks (with $p_{\mathrm{T}} > 1$ GeV), and a total charge of ± 1. Dedicated electron and muon veto algorithms are applied to each τ_{had} candidate.

When different objects selected according to the above criteria overlap with each other geometrically (within $\Delta R = 0.2$), only one of them is considered for further analysis. The overlap is resolved by selecting muon candidates, electron candidates, τ_{had} candidates and jet candidates in this order of priority.

The magnitude and direction of the missing transverse momentum, $E_{\mathrm{T}}^{\mathrm{miss}}$, is reconstructed including contributions from muons and energy deposits in the calorimeters [60]. Clusters of calorimeter-cell energy deposits belonging to jets, τ_{had} candidates, electrons, and photons, as well as cells that are not associated to any object, are treated separately in the $E_{\mathrm{T}}^{\mathrm{miss}}$ calculation. The contributions of muons to $E_{\mathrm{T}}^{\mathrm{miss}}$ are calculated differently for isolated and non-isolated muons, to account for the energy deposited by muons in the calorimeters.

5 The $\mu^+\mu^-$ decay channel

Signal topology and event selection: the signature of the $h/A/H \to \mu^+\mu^-$ decay is a pair of isolated muons with high transverse momenta and opposite charge. In the b-associated production mode, the final state can be further characterised by the presence of one or two low-E_T b-jets. The missing transverse momentum is expected to be small and on the order of the resolution of the $E_{\mathrm{T}}^{\mathrm{miss}}$ measurement. The $\mu^+\mu^-$ decay channel search is complicated by a small branching ratio and considerable background rates.

Events considered in the $\mu^+\mu^-$ analysis must pass a single-muon trigger with a transverse momentum threshold of 18 GeV. At least one reconstructed muon is required to be matched to the η–ϕ region of the trigger object and to have $p_{\mathrm{T}} > 20$ GeV. At least one additional muon of opposite charge and with $p_{\mathrm{T}} > 15$ GeV is required. A muon pair is formed using the two highest-p_{T} muons of opposite charge. This muon pair is required to have an invariant mass greater than 70 GeV. In addition, events are required to have $E_{\mathrm{T}}^{\mathrm{miss}} < 40$ GeV. All muons considered here must be isolated, as defined in section 4.

The large background due to Z/γ^* production can be reduced by requiring that the event contains at least one identified b-jet. Events satisfying this requirement are included in the b-tagged sample, whereas events failing it are included in the b-vetoed sample. The

JHEP02(2013)095

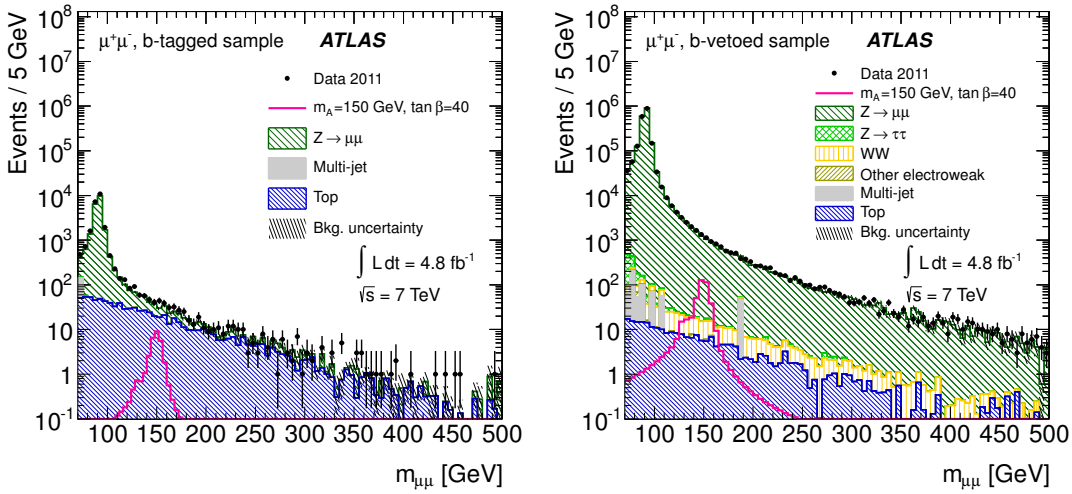

Figure 1. The invariant mass distribution of the two muons of the $h/A/H \to \mu^+\mu^-$ search for the b-tagged (left-hand side) and the b-vetoed samples (right-hand side). The data are compared to the background expectation and a hypothetical MSSM signal ($m_A = 150\,\text{GeV}$, $\tan\beta = 40$). Simulated backgrounds are shown for illustration purposes. The background uncertainties shown here are statistical in nature due to the finite number of simulated events. The contributions of the backgrounds $Z/\gamma^* \to e^+e^-$, W + jets and those of all diboson production processes but WW production are combined and labelled "Other electroweak".

$\mu^+\mu^-$ invariant mass distribution, $m_{\mu\mu}$, is shown separately for the b-tagged and the b-vetoed samples in figure 1. For illustration purposes only, the distributions of simulated backgrounds and an assumed MSSM neutral Higgs boson signal with $m_A = 150\,\text{GeV}$ and $\tan\beta = 40$ are shown in the same figure. A hypothetical signal would be present as narrow peaks on top of the high-mass tail of the Z boson superimposed on a continuous contribution from non-resonant backgrounds such as $t\bar{t}$. The Z/γ^* process contributes to the total background with a relative fraction of about 99% (51%) for the b-vetoed (b-tagged) sample for events in the $m_{\mu\mu}$ range of 110 GeV to 300 GeV, which is most relevant to the Higgs boson searches in this channel. In the b-vetoed sample the remaining non-resonant background is composed of $t\bar{t}$, W^+W^- and $b\bar{b}$ events while $t\bar{t}$ events dominate the non-resonant background in the b-tagged sample.

Background modelling: the background in the $\mu^+\mu^-$ channel is estimated from data. By scanning over the $\mu^+\mu^-$ invariant mass distribution, local sideband fits provide the expected background estimate in the mass region of interest. To this end, a parameterisation of the background shape is fitted to the $\mu^+\mu^-$ invariant mass distribution. Search windows are defined around each of the neutral Higgs bosons and are excluded from the fit. This results in one or two windows due to the mass degeneracy among the Higgs bosons. The widths of the search windows are motivated by the expected signal width for each point in the scanned m_A–$\tan\beta$ grid and account for asymmetries in the signal invariant mass distribution. The upper and lower boundaries of the search windows are defined by the $m_{\mu\mu}$ values where the cross-section predictions of the signal model are 10% of their max-

JHEP02(2013)095

imum. The lower and upper outer boundaries of the sidebands vary between 98–118 GeV and 160–400 GeV, respectively, depending on m_A and m_h.

The parameterisation of the $\mu^+\mu^-$ invariant mass distribution, $f_B(x)$, is given by

$$f_B\left(x\,|N_B, A, B, m_Z, \Gamma_Z, \sigma\right) = N_B \cdot \left[f_Z\left(x\,|A, B, m_Z, \Gamma_Z\right) \otimes \mathcal{F}_{\mathrm{G}}\left(x\,|0, \sigma\right)\right], \tag{5.1}$$

where x is the invariant mass, $\otimes$ the convolution operator and $\mathcal{F}_{\mathrm{G}}\left(x\,|0, \sigma\right)$ the Gaussian distribution with variable x, mean 0 and variance σ^2. The function f_Z describing the Z/γ^* production is

$$f_Z\left(x\,|A, B, m_Z, \Gamma_Z\right) = A\frac{1}{x^2} + B\frac{x^2 - m_Z^2}{\left(x^2 - m_Z^2\right)^2 + m_Z^2\Gamma_Z^2} + \frac{x^2}{\left(x^2 - m_Z^2\right)^2 + m_Z^2\Gamma_Z^2}. \tag{5.2}$$

This is convolved with the Gaussian distribution accounting for the finite mass resolution. The function f_Z is a simplification of the pure γ^* and Z propagators, including Z–γ^* interference contributing to the process $q\bar{q} \to Z/\gamma^* \to \mu^+\mu^-$, and hence in principle only describes the background from Z/γ^* production. The parameterisation f_B is found to be a good approximation of the shape of the total $\mu^+\mu^-$ background even in the b-tagged sample, which has non-negligible contributions from physics processes other than Z/γ^* production.

In total, the fit function, f_B, has six parameters. The natural width of the Z boson, Γ_Z, is fixed to $\Gamma_Z = 2.50\,\mathrm{GeV}$, whereas the remaining parameters are unconstrained. Parameter N_B describes the total normalisation of the curve and parameters A and B represent the relative normalisations of the γ^* and Z–γ^* contributions with respect to the Z term. Finally, m_Z represents the mass of the Z boson and the parameter σ specifies the mean $\mu^+\mu^-$ pair mass resolution.

For every point on the m_A–$\tan\beta$ grid, a binned likelihood fit of f_B to the data is performed to estimate the five unconstrained parameters and consequently the total background estimate.

The background model is validated with χ^2-based goodness-of-fit studies. In addition, the background model is extended by polynomials of different orders to test if additional degrees of freedom change the goodness of the fit, which would hint at problems in the shape modelling. Further validation of the capability of the model to describe the shape of the data is performed by varying the fit ranges for certain mass points and accounting for the fit residuals. The goodness-of-fit studies confirm a good background modelling for both the b-vetoed and the b-tagged sample. The uncertainty on the background estimate is obtained from a variation of the fitted background function within its 68% confidence level (CL) uncertainty band. This results in an uncertainty of 5% (2%) on the expected background yield for the b-tagged (b-vetoed) sample.

Signal modelling: the $h/A/H \to \mu^+\mu^-$ signal is expected to appear as narrow peaks in the $\mu^+\mu^-$ invariant mass distribution, as depicted in figure 1. The resolution in the relevant mass range is typically 2.5% to 3%, and numerous mass points are needed for a complete mass scan. In addition, the influence of $\tan\beta$ on the reconstructed width of the signal invariant mass distribution needs to be taken into account. The natural widths

JHEP02(2013)095

of the MSSM neutral Higgs bosons increase with $\tan\beta$. The reconstructed width can be sensitive to this variation because of the good experimental mass resolution.

To interpolate between the different signal samples obtained from a limited number of simulated signal masses, the signal $\mu^+\mu^-$ invariant mass distribution is parameterised with

$$f_S\left(x\,|N_S, m, \Gamma, \sigma, c, \varsigma\right) = N_S \left[\frac{1}{\left[x^2 - m^2\right]^2 + m^2\Gamma^2} \otimes \mathcal{F}_{\mathrm{G}}\left(x\,|0, \sigma\right) + c \cdot \mathcal{F}_{\mathrm{L}}\left(-x\,|m, \varsigma\right)\right], \tag{5.3}$$

where x represents the $\mu^+\mu^-$ invariant mass. The parameterisation consists of a Breit-Wigner function describing the signal peak convolved with a Gaussian distribution, $\mathcal{F}_{\mathrm{G}}$, accounting for the finite mass resolution and a Landau function, $\mathcal{F}_{\mathrm{L}}$, with low-mass tail which models the asymmetric part of the signal invariant mass distribution.

The function f_S is characterised by six parameters. The width of the Breit-Wigner function, Γ, is fixed to the theoretical predictions calculated with FeynHiggs [31]. The remaining five parameters are unconstrained. The overall normalisation parameter is N_S and c specifies the relative normalisation of the Landau function with respect to the Breit-Wigner function. Parameter m specifies the mean of the Breit-Wigner and the Landau distributions, σ determines the width of the Gaussian distribution and ς represents the scale parameter of the Landau function.

The function f_S is fitted to each signal sample available from simulation. The signal model is validated with Kolmogorov-Smirnov- and χ^2-based goodness-of-fit tests proving a good description of the simulated signal $\mu^+\mu^-$ invariant mass distributions. Each fit results in a set of fitted parameters, $(N_S, m, \sigma, c, \varsigma)$, depending on the point in the m_A–$\tan\beta$ plane. The dependence of this set on m_A and $\tan\beta$ is parameterised with polynomials of different orders. The resulting polynomials provide a set of parameters which in addition to the predicted natural width, Γ, fully define the normalised probability density function for an arbitrary point in the m_A–$\tan\beta$ plane.

This procedure is used to generate invariant mass distributions for signal masses from 120 GeV to 150 GeV in 5 GeV steps and from 150 GeV to 300 GeV in 10 GeV steps, as well as for $\tan\beta$ values from 5 to 70 in steps of 3 or 5. Higgs boson masses below 120 GeV were not considered because the background model does not provide precise estimates in the mass region close to the Z boson peak. For both the b-tagged and the b-vetoed samples the interpolated and normalised probability density functions are obtained separately for the Higgs boson production from gluon-fusion and in association with b-quarks. As for the background, the uncertainty on the signal prediction from the fit is obtained from its 68% CL uncertainty band. The resulting uncertainty is estimated to be 10% to 20% of the signal event yield.

Results: figure 2 compares the data with the background estimate predicted from side-band fits in both the b-tagged and b-vetoed samples for the signal mass point $m_A = 150$ GeV and $\tan\beta = 40$. The data fluctuate around the background prediction leading to local bin-by-bin significances that are typically less than $2\,\sigma$. Table 1 shows the number of observed

JHEP02(2013)095

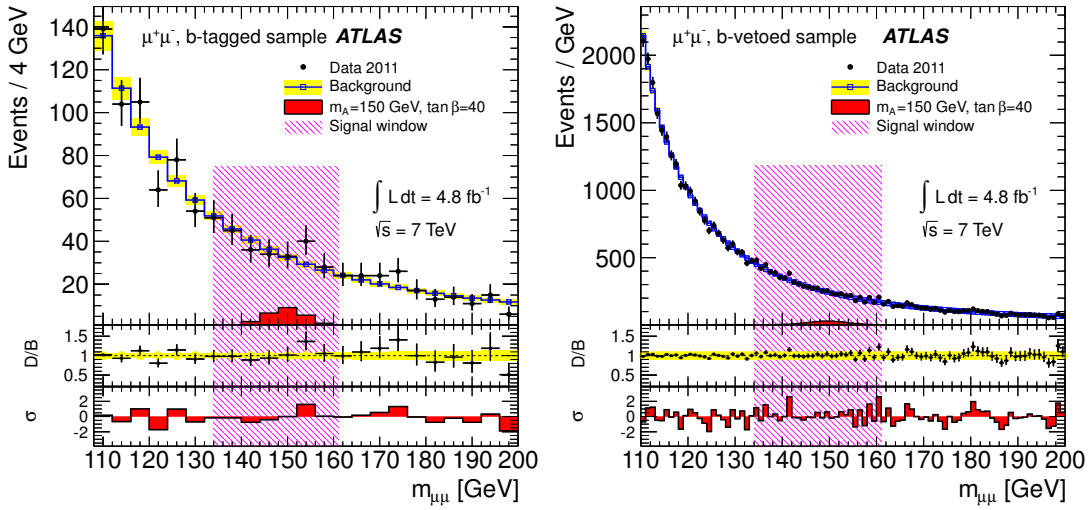

Figure 2. Invariant mass distribution of data and predicted background from sideband fits to the data shown for the signal mass point at $m_A = 150\,\text{GeV}$ and $\tan\beta = 40$ for the b-tagged (left-hand side) and the b-vetoed samples (right-hand side) of the $h/A/H \to \mu^+\mu^-$ final state. The ratio of the data to the predicted background, labelled D/B, and the bin-by-bin significances of the deviations of the data from the background prediction, labelled σ, are shown beneath.

	b-tagged sample	b-vetoed sample
Mass Point	$m_A = 150\,\text{GeV}$	
Fit Range	110–200 GeV	
Background	980 ± 50	35900 ± 600
Signal $m_A = 150\,\text{GeV}, \tan\beta = 40$		
$b\bar{b}(h/A/H \to \mu\mu)$	$28 \pm 2\ ^{+3}_{-4}$	$271 \pm 22\ ^{+31}_{-40}$
$gg \to h/A/H \to \mu\mu$	$2.3 \pm 0.3\ \pm 0.4$	$141 \pm 10\ ^{+22}_{-20}$
Data	985	36044

Table 1. Observed number of data events and the expected number of signal and background events in the $h/A/H \to \mu^+\mu^-$ channel for one of the considered signal mass points. The number of background events is predicted from sideband fits to the $\mu^+\mu^-$ invariant mass distribution in the fit range around the signal mass point $m_A = 150\,\text{GeV}$ for both the $h/A/H \to \mu^+\mu^-$ b-vetoed and b-tagged samples. The number of expected signal events produced in gluon-fusion or in association with b-quarks is shown for $\tan\beta = 40$. The quoted uncertainty for the background estimate is the statistical uncertainty obtained from the fit. For the signal estimate, the uncertainty from the fit is quoted first and then separately the uncertainty from other sources discussed in section 7.

events in the fit range around the mass point $m_A = 150\,\text{GeV}$ compared to the number of background events predicted by the sideband fits. The observed numbers of events are compatible with the expected yield from Standard Model processes within the uncertainties.

JHEP02(2013)095

6 The $\tau^+\tau^-$ decay channel

The $h/A/H \to \tau^+\tau^-$ decay mode is analysed in several categories according to the τ lepton decay final-state combinations. The four decay modes considered here are: $\tau_e\tau_\mu$ (6%), $\tau_e\tau_{\rm had}$ (23%), $\tau_\mu\tau_{\rm had}$ (23%) and $\tau_{\rm had}\tau_{\rm had}$ (42%), where percentages in the parentheses denote the corresponding branching ratios. The combination of $\tau_e\tau_{\rm had}$ and $\tau_\mu\tau_{\rm had}$ is referred to as $\tau_{\rm lep}\tau_{\rm had}$.

6.1 Common background estimation and mass reconstruction techniques

τ-embedded $Z/\gamma^* \to \mu^+\mu^-$ data: $Z/\gamma^* \to \tau^+\tau^-$ events form a largely irreducible background to the Higgs boson signal in all final states. It is not possible to select a $Z/\gamma^* \to \tau^+\tau^-$ control sample which is Higgs boson signal-free. However, $Z/\gamma^* \to \mu^+\mu^-$ events can be selected in data with high purity and without significant signal contamination. Furthermore, the event topology and kinematics are, apart from the τ lepton decays and the different masses of τ leptons and muons, identical to those of $Z/\gamma^* \to \tau^+\tau^-$ events. Therefore $Z/\gamma^* \to \mu^+\mu^-$ events are selected in data and modified using a τ-embedding technique, in which muons are replaced by simulated τ leptons. The hits of the muon tracks and the associated calorimeter cells in a cone with radius parameter $\Delta R = 0.1$ around the muon direction are removed from the data event and replaced by the detector response from a simulated $Z/\gamma^* \to \tau^+\tau^-$ event with the same kinematics. The event reconstruction is performed on the resulting hybrid event. Only the τ decays and their detector response are taken from the simulation, whereas the underlying event kinematics and the associated jets are taken from the data event. The procedure treats consistently the effect of τ polarisation and spin correlations. The event yield of the embedded sample after the selection of the τ decay products is normalised to the corresponding event yield obtained in a simulated $Z/\gamma^* \to \tau^+\tau^-$ sample. This procedure has been validated as described in references [7, 61].

Systematic uncertainties on the normalisation and shape of the embedded sample are derived by propagating variations of the $Z/\gamma^* \to \mu^+\mu^-$ event selection and the muon energy subtraction procedure through the τ-embedding process. Additional uncertainties are assigned due to the use of the $Z/\gamma^* \to \tau^+\tau^-$ cross-section and Monte Carlo acceptance prediction in determining the τ-embedded $Z/\gamma^* \to \mu^+\mu^-$ sample normalisation. These theoretical uncertainties are described in section 7.

Jets misidentified as hadronic τ decays: a fraction of jets originating from quarks or gluons are misidentified as $\tau_{\rm had}$ candidates. It has been shown in reference [62] that this misidentification fraction is higher in simulated samples than in data. To account for this difference, the Monte Carlo background estimate is corrected based on control samples. Details are presented for each decay channel separately.

The *ABCD* background estimation method: the estimation of the background from multi-jet processes is done from data using the *ABCD* method for all $\tau^+\tau^-$ channels. Two uncorrelated variables are chosen to define four data regions, named A, B, C and D, such that one variable separates A and B from C and D, while the other separates A and C from B and D. The signal region is labelled A, and the other regions are dominated by

JHEP02(2013)095

background from multi-jet processes. An estimate of the background from these processes in the signal region, n_A, is:

$$n_A = n_B \times \frac{n_C}{n_D} \equiv n_B \times r_{C/D}, \tag{6.1}$$

where n_B, n_C and n_D denote the populations of regions B, C and D, respectively. The populations of the B, C and D regions may need to be corrected by subtracting the estimated number of events that come from processes other than multi-jet production. This estimate is generally obtained from simulation.

$\tau^+\tau^-$ mass reconstruction: the invariant mass of the $\tau^+\tau^-$ pair cannot be reconstructed directly due to the presence of neutrinos from the τ lepton decays. Therefore, a technique known as the Missing Mass Calculator (MMC) is used to reconstruct the Higgs boson candidate mass [63]. This algorithm assumes that the missing transverse momentum is due entirely to the neutrinos, and performs a scan over the angles between the neutrinos and the visible τ lepton decay products. For leptonic τ decays, the scan also includes the invariant mass of the two neutrinos. At each point, the $\tau^+\tau^-$ invariant mass is calculated, and the most likely value is chosen by weighting each solution according to probability density functions that are derived from simulated τ lepton decays. This method provides a 13% to 20% resolution in the invariant mass, with an efficiency of 99% for the scan to find a solution.

6.2 The $h/A/H \to \tau_e\tau_\mu$ decay channel

Signal topology and event selection: events in this channel must satisfy either a single-electron, single-muon or combined electron-muon trigger. The single-lepton triggers have p_{T} thresholds of 20 GeV or 22 GeV for electrons, depending on the run period, and 18 GeV for muons, while the combined trigger has a threshold of 10 GeV for the electron and 6 GeV for the muon. Exactly one isolated electron and one isolated muon of opposite electric charge are required, and the lepton pair must have an invariant mass exceeding 30 GeV. The p_{T} thresholds are 15 GeV for electrons and 10 GeV for muons in cases where the event is selected by the combined electron-muon trigger. These thresholds are raised to 24 GeV for electrons and 20 GeV for muons in cases where the event is selected by a single-lepton trigger only.

The event sample is then split according to its jet flavour content. Events containing exactly one identified b-jet are included in the b-tagged sample. This is based on a b-jet identification criterion with 75% efficiency in $t\bar{t}$ events. Events without an identified b-jet are included in the b-vetoed sample. The scalar sum of the lepton transverse momenta and missing transverse momentum is required to fulfil the following condition to reduce top quark and diboson backgrounds: $E_{\mathrm{T}}^{\mathrm{miss}} + p_{\mathrm{T},e} + p_{\mathrm{T},\mu} < 125\,\mathrm{GeV}$ ($< 150\,\mathrm{GeV}$) for the b-tagged (b-vetoed) sample. In order to further suppress these backgrounds and $W \to \ell\nu$ events, the opening angle between the two lepton candidates in the transverse plane must satisfy the condition $\Delta\phi_{e\mu} > 2.0$ (> 1.6) for the b-tagged (b-vetoed) sample. In addition, the combination of the transverse opening angles between the lepton directions and the direction of $E_{\mathrm{T}}^{\mathrm{miss}}$ is required to satisfy the condition $\sum_{\ell=e,\mu} \cos\Delta\phi_{E_{\mathrm{T}}^{\mathrm{miss}},\ell} > -0.2$

JHEP02(2013)095

Region	Charge correlation	Lepton isolation requirement
A (Signal Region)	Opposite sign	isolated
B	Same sign	isolated
C	Opposite sign	anti-isolated
D	Same sign	anti-isolated

Table 2. Control regions for the estimation of the multi-jet background for the $h/A/H \to \tau_e\tau_\mu$ and $h/A/H \to \tau_{\text{lep}}\tau_{\text{had}}$ samples: events are categorised according to the charge product of the two τ leptons and the lepton isolation requirement. In the $h/A/H \to \tau_{\text{lep}}\tau_{\text{had}}$ channel isolation refers to the isolation of the electron or muon and in the $h/A/H \to \tau_e\tau_\mu$ channel both the electron and muon are required to be isolated or anti-isolated, respectively.

(> -0.4) for the b-tagged (b-vetoed) sample. Finally, the scalar sum of the transverse energies of all jets, H_{T}, is restricted to be below 100 GeV in the b-tagged sample to further suppress backgrounds containing a higher multiplicity of jets, or jets with higher transverse momenta, than expected from the signal processes. Jets with $|\eta| < 4.5$ and $E_T > 20$ GeV are used to calculate the value of H_{T}.

Estimation of the $Z/\gamma^* \to \tau^+\tau^-$ background: the $Z/\gamma^* \to \tau^+\tau^-$ background is estimated by using the τ-embedded $Z/\gamma^* \to \mu^+\mu^-$ event sample outlined in section 6.1. The use of multiple triggers with different p_{T} thresholds has an effect on the lepton transverse momentum spectra, which is accurately reproduced by the trigger simulation. However, in the τ-embedded $Z/\gamma^* \to \mu^+\mu^-$ data there is no simulation of the trigger response for the decay products of the τ leptons. This has an impact on the MMC mass distribution in the τ-embedded $Z/\gamma^* \to \mu^+\mu^-$ data, which is comparable to the statistical uncertainty in the b-vetoed sample, and negligible in the b-tagged sample. For this reason the trigger selection is emulated for the b-vetoed sample such that the trigger effect is adequately described. This emulation is based on the p_{T}-dependent trigger efficiencies obtained from data.

Estimation of the $t\bar{t}$ background: the contribution of $t\bar{t}$ production is extrapolated from control regions which have purities of 90% (b-tagged sample) and 96% (b-vetoed sample). The selection criteria for these control regions are identical to the respective signal regions with two exceptions: at least two identified b-jets are required, and the selection $H_{\text{T}} < 100$ GeV is not applied. The multi-jet contributions to these control regions are estimated from data with the $ABCD$ method; the other non-$t\bar{t}$ contributions are taken from simulation. The uncertainty on the normalisation obtained in this manner is 15% (30%) in the b-tagged (b-vetoed) sample, primarily due to uncertainties on the b-tagging efficiency and jet energy scale.

Estimation of the multi-jet background: the multi-jet background is estimated using the $ABCD$ method, by splitting the event sample into four regions according to the charge product of the $e\mu$ pair and the isolation requirements on the electron and muon. These requirements are summarised in table 2.

The systematic uncertainty of this method has been estimated by considering the stability of the ratio $r_{C/D}$ in regions where the isolation requirements are varied, or where only

JHEP02(2013)095

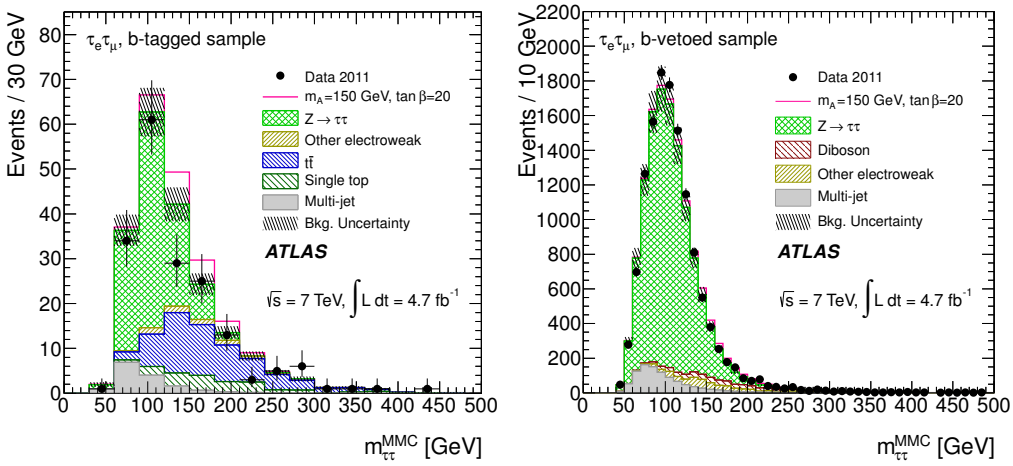

Figure 3. MMC mass distributions for the $h/A/H \to \tau_e\tau_\mu$ final state. The MMC mass, $m_{\tau\tau}^{\mathrm{MMC}}$, is shown for the b-tagged (left-hand side) and b-vetoed samples (right-hand side). The data are compared to the background expectation and an added hypothetical MSSM signal ($m_A = 150\,\mathrm{GeV}$ and $\tan\beta = 20$). The background uncertainties include statistical and systematic uncertainties. The contributions of the backgrounds $Z/\gamma^* \to e^+e^-$, $Z/\gamma^* \to \mu^+\mu^-$ and W + jets are combined and labelled "Other electroweak"; in the case of the b-tagged samples the contributions of diboson production processes are included as well. Background contributions from top quarks are included in "Other electroweak" for the b-vetoed sample.

the muon is required to fail the isolation. The resulting uncertainty on the normalisation is 14% (23%) in the b-tagged (b-vetoed) sample.

Smaller backgrounds from W + jets, $Z/\gamma^* \to e^+e^-$, $Z/\gamma^* \to \mu^+\mu^-$, diboson, and single-top processes are estimated from simulation.

Results: the number of observed $\tau_e\tau_\mu$ events in data, along with predicted event yields from background processes, is shown in table 3. The observed event yield is compatible with the expected event yield from Standard Model processes within the uncertainties. The MMC mass distributions for these events are shown in figure 3.

6.3 The $h/A/H \to \tau_{\mathrm{lep}}\tau_{\mathrm{had}}$ decay channel

Signal topology and event selection: events in the $h/A/H \to \tau_{\mathrm{lep}}\tau_{\mathrm{had}}$ channel are selected using a single-lepton trigger with transverse momentum thresholds of 20 GeV or 22 GeV for electrons, depending on the run period, and 18 GeV for muons. Each event must contain one isolated electron with $p_{\mathrm{T}} > 25\,\mathrm{GeV}$ or one isolated muon with $p_{\mathrm{T}} > 20\,\mathrm{GeV}$. Events containing additional electrons or muons with transverse momenta greater than 15 GeV or 10 GeV, respectively, are rejected in order to obtain an orthogonal selection to those used in the $\tau_e\tau_\mu$ and $\mu^+\mu^-$ channels. One τ_{had} with a charge of opposite sign to the selected electron or muon is required. The τ_{had} identification criterion in use is the one with medium efficiency as introduced in section 4. The transverse mass of the lepton and the missing transverse momentum, m_{T}, is required to be less than 30 GeV, to reduce contamination from W + jets and $t\bar{t}$ background processes. Here the transverse mass is

JHEP02(2013)095

	b-tagged sample		b-vetoed sample	
$Z/\gamma^* \to \tau^+\tau^-$	109	± 12	11000	± 1000
$W+$jets	1.2	$^{+1.1}_{-0.9}$	111	± 23
$Z/\gamma^* \to \ell^+\ell^-$	1.1	± 0.8	196	$^{+22}_{-23}$
$t\bar{t}$	56	$^{+11}_{-9}$	150	$^{+60}_{-50}$
Single top	16	$^{+3}_{-4}$	35	± 5
Diboson	3.9	± 0.7	470	± 50
Multi-jet	15	± 11	980	± 230
Total	201	$^{+20}_{-19}$	13000	± 1000
Signal $m_A = 150\,\text{GeV}, \tan\beta = 20$				
$b\bar{b}(h/A/H \to \tau\tau)$	18	$^{+4}_{-5}$	270	$^{+40}_{-50}$
$gg \to h/A/H \to \tau\tau$	2.3	± 0.8	143	$^{+23}_{-21}$
Data	181		12947	

Table 3. The number of events observed in data and the expected number of signal and background events of the $h/A/H \to \tau_e\tau_\mu$ channel. Simulated event yields are normalised to the integrated luminosity of the data sample, $4.7\,\text{fb}^{-1}$. The predicted signal event yields correspond to a parameter choice of $m_A = 150\,\text{GeV}$ and $\tan\beta = 20$ and include both the b-associated and the gluon-fusion production processes.

defined as:

$$m_{\text{T}} = \sqrt{2p_{\text{T}}^{\text{lep}} E_{\text{T}}^{\text{miss}} \left(1 - \cos\Delta\phi\right)}\,, \tag{6.2}$$

where $p_{\text{T}}^{\text{lep}}$ denotes the transverse momentum of the electron or muon and $\Delta\phi$ the angle between $p_{\text{T}}^{\text{lep}}$ and $E_{\text{T}}^{\text{miss}}$.

After imposing these selection criteria, the resulting event sample is split into two categories depending on whether or not the highest-E_T jet with $|\eta| < 2.5$ is identified as a b-jet. Events are included in the b-tagged sample if the highest-E_T jet is identified as a b-jet and its E_T is in the range of 20 GeV to 50 GeV. Events are included in the b-vetoed sample if the highest-E_T jet fails the b-jet identification criterion and the event has $E_{\text{T}}^{\text{miss}} > 20\,\text{GeV}$.

Estimation of the W + jets background: W+jets events that pass the event selection criteria up to the m_{T} requirement consist primarily of events in which the selected lepton originates from the W decay and a jet is misidentified as a τ_{had}. To ensure a proper estimation of the jet-to-τ_{had} misidentification rate, the $W+$jets background normalisation is corrected using control regions with high purity in $W+$jets events defined by requiring high transverse mass: $70\,\text{GeV} < m_{\text{T}} < 110\,\text{GeV}$. Separate control regions are used for the $\tau_e\tau_{\text{had}}$ and $\tau_\mu\tau_{\text{had}}$ samples, as the kinematic selections are different. The correction factors derived from these control regions are $f_W^e = 0.587 \pm 0.009$ for the electron channel and $f_W^\mu = 0.541 \pm 0.008$ for the muon channel, where the quoted uncertainties are statistical. The relative systematic uncertainty is estimated to be 5% by varying the m_{T} boundary

JHEP02(2013)095

definition of the control region. The correction factors have been derived separately for the b-tagged and b-vetoed samples; the numbers are in agreement between the two cases, but for the b-tagged sample the statistical uncertainty is 17%. This statistical uncertainty is considered as an additional systematic uncertainty in the b-tagged sample analysis.

Estimation of the $Z/\gamma^* \to \tau^+\tau^-/e^+e^-/\mu^+\mu^-$ background: the $Z/\gamma^* \to \tau^+\tau^-$ background is estimated using the τ-embedded $Z/\gamma^* \to \mu^+\mu^-$ sample outlined in section 6.1. The jet activity in the embedded events is independent of the Z boson decay mode. Taking advantage of this feature, the embedding sample is also used to validate the simulated $Z/\gamma^* \to e^+e^-$ and $Z/\gamma^* \to \mu^+\mu^-$ background samples for the correct b-jet fraction, which may affect the background estimation after imposing the b-tag requirement. Correction factors are derived by comparing τ-embedded $Z/\gamma^* \to \mu^+\mu^-$ events with simulated $Z/\gamma^* \to \tau^+\tau^-$ events before and after the b-tagged sample selection. The correction factors are calculated to be $f^e_{Zb} = 1.08 \pm 0.23$ and $f^\mu_{Zb} = 1.11 \pm 0.13$ for the electron and muon channels, respectively, where the quoted uncertainties are statistical. The effect on these correction factors from the $t\bar{t}$ contribution in the control region is studied by removing the 50 GeV maximum E_T requirement on the b-jet. A 7% systematic uncertainty is obtained. These factors are applied to the simulated $Z/\gamma^* \to e^+e^-$ and $Z/\gamma^* \to \mu^+\mu^-$ background samples passing the b-tagged sample selection.

Estimation of the $t\bar{t}$ background: the simulated $t\bar{t}$ samples are normalised from data using a top-enriched control region. This control region is defined by applying the $\tau_{\text{lep}}\tau_{\text{had}}$ selection criteria up to the requirement of a $e\tau_{\text{had}}$ or $\mu\tau_{\text{had}}$ pair in the event, with no requirement on the transverse mass. The highest-E_T jet in the event must be identified as a b-jet, with E_T in the range 50 GeV to 150 GeV, and a second highest-E_T jet must satisfy the same b-jet identification requirement. This results in a control region with a purity of $t\bar{t}$ events over 90% and negligible signal contribution. The $t\bar{t}$ correction factor is derived in a manner similar to that of the W + jets correction factor, and a value of $f_{t\bar{t}} = 0.88 \pm 0.04$ (stat.) ± 0.14 (syst.) is obtained with the systematic uncertainty due primarily to the b-jet identification efficiency.

Estimation of the multi-jet background: for the multi-jet background estimation, the $ABCD$ method is used by defining four regions according to whether the charge of the τ jet and lepton have opposite sign or same sign, and whether the selected lepton passes or fails the isolation criteria. These requirements are summarised in table 2. In regions C and D the contribution from processes other than the multi-jet background is negligible, while in region B there is a significant contribution from other backgrounds, in particular Z/γ^* +jets and W + jets, which is subtracted from the data sample using estimates from simulation. The systematic uncertainty on the predicted event yield is estimated by varying the definitions of the regions used, and by testing the stability of the $r_{C/D}$ ratio across the $m^{\text{MMC}}_{\tau\tau}$ range. The resulting uncertainty is 7.5% in the $\tau_\mu\tau_{\text{had}}$ channel and 15% in the $\tau_e\tau_{\text{had}}$ channel.

Results: the number of observed $\tau_{\text{lep}}\tau_{\text{had}}$ events in data, along with predicted event yields from background processes, are shown in table 4. The observed event yields are compatible

JHEP02(2013)095

	Muon Channel ($\tau_\mu\tau_{\rm had}$)			
	b-tagged sample		b-vetoed sample	
$Z/\gamma^* \to \tau^+\tau^-$	86	± 15	4800	± 700
W + jets	19	$^{+6}_{-8}$	780	$^{+100}_{-140}$
$Z/\gamma^* \to \ell^+\ell^-$	8	$^{+5}_{-4}$	350	$^{+100}_{-90}$
Top	14.5	$^{+3.5}_{-2.7}$	105	$^{+20}_{-21}$
Diboson	0.8	± 0.4	38	$^{+6}_{-5}$
Multi-Jet	51	± 11	580	$^{+140}_{-130}$
Total	180	± 20	6600	± 800
Signal $m_A = 150\,\text{GeV}, \tan\beta = 20$				
$b\bar{b}(h/A/H \to \tau\tau)$	20	$^{+5}_{-6}$	174	$^{+27}_{-35}$
$gg \to h/A/H \to \tau\tau$	1.2	± 0.6	115	± 16
Data	202		6424	

	Electron Channel ($\tau_e\tau_{\rm had}$)			
	b-tagged sample		b-vetoed sample	
$Z/\gamma^* \to \tau^+\tau^-$	42	± 20	2700	± 500
W + jets	18	$^{+9}_{-12}$	740	$^{+110}_{-160}$
$Z/\gamma^* \to \ell^+\ell^-$	19	± 10	700	$^{+350}_{-270}$
Top	15.1	± 3.0	106	$^{+20}_{-21}$
Diboson	1.0	$^{+0.4}_{-0.5}$	29	$^{+5}_{-4}$
Multi-Jet	60	± 15	920	$^{+230}_{-240}$
Total	154	± 30	5200	± 600
Signal $m_A = 150\,\text{GeV}, \tan\beta = 20$				
$b\bar{b}(h/A/H \to \tau\tau)$	15	$^{+3}_{-5}$	138	$^{+22}_{-29}$
$gg \to h/A/H \to \tau\tau$	1.2	$^{+0.6}_{-0.4}$	99	$^{+15}_{-14}$
Data	175		5034	

Table 4. The number of events observed in data and the expected number of signal and background events for the $h/A/H \to \tau_{\rm lep}\tau_{\rm had}$ channel. Simulated event yields are normalised to the integrated luminosity of the data sample, $4.7\,\text{fb}^{-1}$. The predicted signal event yields correspond to the parameter choice $m_A = 150\,\text{GeV}$ and $\tan\beta = 20$ and include both the b-associated and the gluon-fusion production processes.

with the expected yields from Standard Model processes within the uncertainties. The MMC mass distributions for these events, with $\tau_\mu\tau_{\rm had}$ and $\tau_e\tau_{\rm had}$ statistically combined, are shown in figure 4.

JHEP02(2013)095

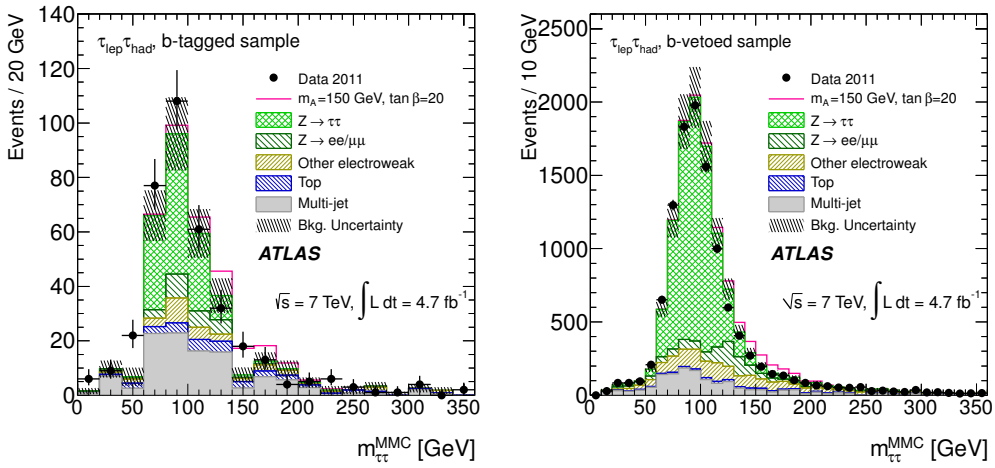

Figure 4. MMC mass distributions for the $h/A/H \to \tau_{\text{lep}}\tau_{\text{had}}$ final state. The MMC mass, $m_{\tau\tau}^{\text{MMC}}$, is shown for the b-tagged (left-hand side) and b-vetoed samples (right-hand side) for the combined $\tau_e\tau_{\text{had}}$ and $\tau_\mu\tau_{\text{had}}$ samples. The data are compared to the background expectation and a hypothetical MSSM signal ($m_A = 150\,\text{GeV}$ and $\tan\beta = 20$). The background uncertainties include statistical and systematic uncertainties. The contributions of the diboson and $W+\text{jets}$ background processes are combined and labelled "Other electroweak".

6.4 The $h/A/H \to \tau_{\text{had}}\tau_{\text{had}}$ decay channel

Signal topology and event selection: events in this channel are selected by a di-τ_{had} trigger with transverse momentum thresholds of 29 GeV and 20 GeV for the two τ_{had} candidates. Events containing identified electrons or muons with transverse momenta above 15 GeV or 10 GeV, respectively, are vetoed. These vetoes suppress background events and ensure that the channels are statistically independent. Two τ_{had} candidates with opposite-sign charges are required, one passing the tight τ_{had} identification requirements and the second passing the medium criteria. These two leading τ_{had} candidates are required to match the reconstructed τ_{had} trigger objects each within a cone with radius parameter $\Delta R < 0.2$. These two τ_{had} candidates are required to have transverse momenta above 45 GeV and 30 GeV, respectively. These values are chosen such that the plateau of the trigger turn-on curve is reached and the electroweak and multi-jet backgrounds are suppressed effectively. The missing transverse momentum is required to be above 25 GeV to account for the presence of neutrinos originating from the τ decays and to suppress multi-jet background.

The selected events are split into a b-tagged sample and a b-vetoed sample to exploit the two dominant production mechanisms for neutral Higgs bosons in the MSSM. Events in which the leading jet is identified as a b-jet are included in the b-tagged sample. The transverse momentum of this jet is restricted to the range of 20 GeV to 50 GeV to reduce the $t\bar{t}$ background. Events without jets, or in which the leading jet is not identified as a b-jet, are included in the b-vetoed sample. Due to the higher background levels in this sample, the threshold on the transverse momentum of the leading τ_{had} candidate is raised to 60 GeV.

JHEP02(2013)095

Identification efficiency and misidentification corrections for hadronic τ decays: the τ_{had} identification efficiencies, the τ_{had} trigger efficiencies and the corresponding misidentification probabilities are corrected for differences observed between data and simulation. For the di-τ_{had} trigger it is assumed that these identification and misidentification efficiencies can be factorised into the efficiencies of the corresponding single-τ_{had} triggers with appropriate transverse momentum requirements. This factorisation is validated using a simulated event sample. The single-τ_{had} trigger efficiency for real hadronically decaying τ leptons with respect to the offline τ_{had} selection was measured using a tag-and-probe analysis with $Z \to \tau_\mu \tau_{\text{had}}$ data. A correction factor for the simulation was derived as a function of the transverse momentum of each of the two τ_{had} candidates, and each event was weighted by the product of these factors. The probability to misidentify a jet as a τ_{had} is extracted for both the trigger and the τ_{had} identification algorithm by analysing jets in a high-purity $W(\to \mu\nu)$+jets sample. A correction factor derived on the basis of these probabilities is applied to the simulation when a jet is misidentified as a τ_{had}. The statistical and systematic uncertainty of these correction factors leads to an uncertainty of 21% on the W + jets background and 4% to 6% on the $t\bar{t}$ background.

Estimation of the $Z/\gamma^* \to \tau^+\tau^-$ and $W(\to \tau\nu)$+jets backgrounds: the estimates of the $Z/\gamma^* \to \tau^+\tau^-$ and $W(\to \tau\nu)$+jets backgrounds are taken from simulation and are validated using τ-embedded $Z/\gamma^* \to \mu^+\mu^-$ and $W(\to \mu\nu)$+jets samples. The τ-embedded $Z/\gamma^* \to \mu^+\mu^-$ data are used to validate the simulation, rather than to provide the main estimate for the $Z/\gamma^* \to \tau^+\tau^-$ background, in the $h/A/H \to \tau_{\text{had}}\tau_{\text{had}}$ channel. The di-τ_{had} trigger is not modelled in the τ-embedded $Z/\gamma^* \to \tau^+\tau^-$ data, making it difficult to apply the embedding technique. Correction factors for the efficiency of the b-jet identification requirement on the leading jet are derived in a way equivalent to that described in section 6.3. For the Z/γ^*+jets background a factor of $f_{Zb} = 1.24 \pm 0.34$ (stat.) is derived by comparing the simulated and embedded $Z/\gamma^* \to \tau^+\tau^-$ samples. With the embedded $W(\to \tau\nu)$+jets sample, no such correction factor may be derived in this way as the contamination from $t\bar{t}$ events is quite significant once the b-jet identification requirements are applied. Instead, the procedure in section 6.3 is applied with the selection of this channel. A correction factor of $f_{Wb} = 1.00 \pm 0.31$ (stat.) is derived for $W(\to \tau\nu)$+jets events. The correction factors for the b-vetoed sample are found to be close to unity and uncertainties are negligible, hence no correction is applied.

Estimation of the multi-jet background: the multi-jet background is estimated using the $ABCD$ method, by splitting the event sample into four regions based on the charge product of the two leading τ_{had} candidates and whether the nominal τ_{had} identification requirements of these two τ_{had} candidates are met. These variables can be assumed to be uncorrelated for multi-jet events. Table 5 illustrates the definition of the four regions.

The shape of the MMC mass distribution for the multi-jet background in the signal region is taken from region C for the b-vetoed sample and from region B for the b-tagged sample. Contributions from electroweak backgrounds are subtracted from each control region using simulation. The uncertainties on these backgrounds lead to uncertainties on the multi-jet estimate of 7% for the b-tagged sample and 5% for the b-vetoed sample.

JHEP02(2013)095

Region	Charge correlation	Hadronic τ decay identification requirement
A (Signal Region)	Opposite sign	Pass
B	Same sign	Pass
C	Opposite sign	Fail
D	Same sign	Fail

Table 5. Control regions for the estimation of the multi-jet background for the $h/A/H \to \tau_{\text{had}}\tau_{\text{had}}$ selection: Events are categorised according to the product of the electric charges of the two τ_{had} candidates and the τ_{had} identification. "Pass" refers to one τ_{had} candidate passing the tight and the other τ_{had} candidate passing the medium identification selection. "Fail" refers to all events in which the two τ_{had} pass the loose identification selection but do not satisfy the selection of the "Pass" category.

	b-tagged sample		b-vetoed sample	
Multi-jet	19	± 5	870	± 50
$Z/\gamma^* \to \tau^+\tau^-$	4.0	± 3.0	300	$^{+80}_{-70}$
W + jets	0.5	$^{+0.5}_{-0.4}$	50	± 20
Top	1.7	± 0.6	11.2	± 2.2
Diboson	0.01	± 0.04	4.9	± 1.0
Total	25	± 5	1200	$^{+80}_{-70}$
Signal $m_A = 150\,\text{GeV}, \tan\beta = 20$				
$b\bar{b}(h/A/H \to \tau\tau)$	7.7	± 3.4	73	± 21
$gg \to h/A/H \to \tau\tau$	0.5	± 0.2	47	± 11
Data	27		1223	

Table 6. The observed number of events in data and the expected number of signal and background events for the $h/A/H \to \tau_{\text{had}}\tau_{\text{had}}$ channel. Simulated event yields are normalised to the total integrated luminosity, $4.7\,\text{fb}^{-1}$. The data are compared to the background expectation and an added hypothetical MSSM signal ($m_A = 150\,\text{GeV}$ and $\tan\beta = 20$). Because of the subtraction of the $Z/\gamma^* \to \tau^+\tau^-$ background in the control regions used in the multi-jet background estimation the uncertainties of the $Z/\gamma^* \to \tau^+\tau^-$ and the multi-jet backgrounds are anti-correlated.

Results: the number of observed $\tau_{\text{had}}\tau_{\text{had}}$ events in data, along with predicted event yields from background processes, is shown in table 6. The observed event yields are compatible with the expected yields from Standard Model processes within the uncertainties. The MMC mass distributions for these events are shown in figure 5.

7 Systematic uncertainties

Data-driven background estimation: where possible, event yields and mass distributions for the background are estimated using control samples in data. The specific techniques and their associated uncertainties have been presented in the relevant sections. The effect of these uncertainties on the predicted background event yield is less than 5% for

JHEP02(2013)095

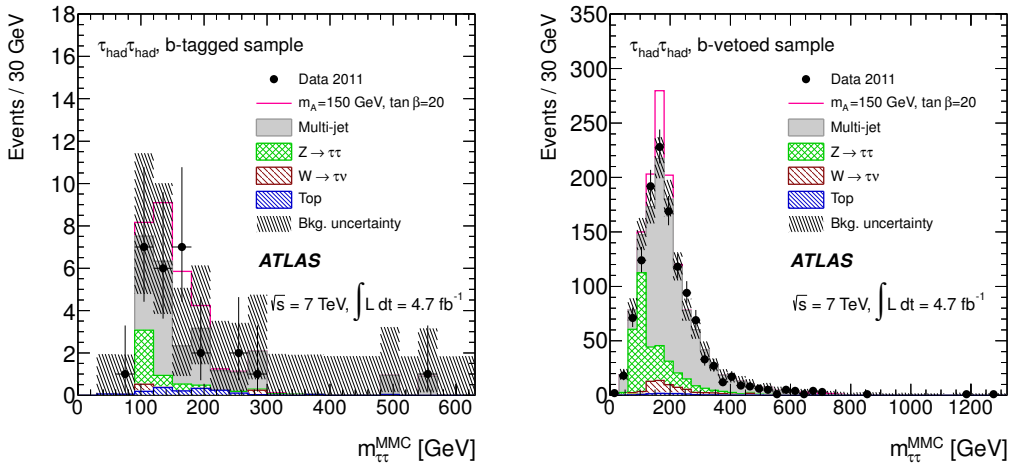

Figure 5. MMC mass distributions for the $h/A/H \to \tau_{\rm had}\tau_{\rm had}$ final state. The MMC mass , $m_{\tau\tau}^{\rm MMC}$, is shown for the b-tagged (left-hand side) and b-vetoed samples (right-hand side). The data are compared to the background expectation and an added hypothetical MSSM signal ($m_A = 150\,\text{GeV}$ and $\tan\beta = 20$). The background uncertainties include statistical and systematic uncertainties.

the $\mu^+\mu^-$ channels and less than 15% for the $\tau^+\tau^-$ channels, and is usually small compared to the systematic uncertainties from the simulated samples.

Cross-section for signal and background samples: the uncertainties on the signal cross-sections are estimated to be 10% to 20%, depending on the values of m_A and $\tan\beta$, for both gluon-fusion and b-associated Higgs boson production [32]. An uncertainty of 5% is assumed on the cross-sections for W and Z boson background production [64, 65]. Uncertainties due to the parton distribution functions and the renormalisation and factorisation scales are included in these estimates.

Acceptance modelling for simulated samples: the uncertainty on the acceptance from the parameters used in the event generation of signal and background samples is also considered. This is done by evaluating the change in kinematic acceptance after varying the relevant scale parameters, parton distribution function choices, and if applicable, conditions for the matching of the partons used in the fixed order calculation and the parton shower. Furthermore, the effects of different tunes of the underlying event activity are considered. The resulting uncertainties are typically 2% to 20%, depending on the sample and the channel considered.

Electron and muon identification and trigger: the uncertainties on electron or muon trigger and identification efficiencies are determined from data using samples of W and Z decays [53, 54]. The trigger efficiency uncertainties are below about 1%. The identification efficiency uncertainties are between 3% and 6% for electrons and below 1.8% for muons. The total effect of these uncertainties on the event yield is no greater than 4% in any channel.

Hadronic τ identification and trigger: the uncertainties related to hadronic τ trigger and identification efficiencies are also studied with data [59]. The di-$\tau_{\rm had}$ trigger efficiency

JHEP02(2013)095

used in the $\tau_{\text{had}}\tau_{\text{had}}$ channel has an uncertainty of 2% to 7%. The identification efficiency uncertainty for hadronic τ decays is about 4% for reconstructed τ_{had} p_{T} above 22 GeV and 8% otherwise. These uncertainties are most important in the $\tau_{\text{had}}\tau_{\text{had}}$ channel, where the effect on the estimated signal yield reaches 11%.

***b*-jet identification:** the b-jet identification efficiency and the misidentification probabilities for jets other than b-jets have been measured in data [58, 66]. The associated uncertainties are treated separately for all jet flavours and depend on jet E_T and η. Typical uncertainty values are around 5% for b-jets and between 20% and 30% for other jets, leading to a total uncertainty close to 5% on the event yield in the b-tagged channels.

Energy scale and resolution: the uncertainty on the acceptance due to the energy measurement uncertainty in the calorimeter is considered for each identified object corresponding to the clusters in the calorimeters. For the clusters identified as electrons, typically a 1% (3%) energy scale uncertainty is assigned for the barrel (end-cap) region [53]. The energy scale uncertainties for clusters identified as hadronic τ decays and jets are treated as being fully correlated, and are typically around 3% [57, 59]. The uncertainty in the muon energy scale is below 1%. The acceptance uncertainty due to the jet energy resolution, which affects the p_{T} thresholds used to define the b-tagged and b-vetoed samples, is typically less than 1%. The systematic uncertainty due to the energy scales of electrons, muons, hadronic τ decays and jets is propagated to the $E_{\text{T}}^{\text{miss}}$ vector. Additional uncertainties due to different pile-up conditions in data and simulation are also considered.

The uncertainty on the acceptance due to the energy scale and resolution variations reaches up to 37% for signal in the $\tau_{\text{had}}\tau_{\text{had}}$ b-tagged channel, but is usually less than 10% for channels with fewer τ_{had}.

Luminosity: the simulated sample event yield is normalised to the integrated luminosity of the data, which is measured [67, 68] to be 4.7 fb^{-1} and 4.8 fb^{-1} for the $\tau^+\tau^-$ and $\mu^+\mu^-$ channels, respectively, and has an uncertainty of 3.9%. This is applicable to all signal and background processes which are not normalised using data-driven methods.

8 Statistical analysis

The statistical analysis of the data employs a binned likelihood function. Each one of the $\mu\mu$, $\tau_e\tau_\mu$, $\tau_e\tau_{\text{had}}$, $\tau_\mu\tau_{\text{had}}$ and $\tau_{\text{had}}\tau_{\text{had}}$ final states is split into a b-tagged and a b-vetoed sample. The likelihood in each category is a product over bins in the distributions of the MMC mass in the signal and control regions.

The expected number of events for signal (s_j) and background (b_j), as well as the observed number of events (N_j) in each bin of the mass distributions, enter in the definition of the likelihood function $\mathcal{L}(\mu, \boldsymbol{\theta})$. A "signal strength" parameter (μ) scales the expected signal in each bin. The value $\mu = 0$ corresponds to the background-only hypothesis, while $\mu = 1$ corresponds to the signal-plus-background hypothesis with all Higgs bosons having the masses and cross-sections specified by the point considered in the m_A–$\tan\beta$ plane for

JHEP02(2013)095

the MSSM exclusion limit. Signal and background predictions depend on systematic uncertainties that are parameterised by nuisance parameters, $\boldsymbol{\theta}$, which in turn are constrained using Gaussian functions, $\mathcal{F}_{\mathrm{G}}$, so that

$$\mathcal{L}(\mu, \boldsymbol{\theta}) = \prod_{\substack{j = \text{bin and} \\ \text{category}}} \mathcal{F}_{\mathrm{P}}\left(N_j \,|\, \mu \cdot s_j + b_j\right) \prod_{\theta_i} \mathcal{F}_{\mathrm{G}}\left(\theta_i \,|\, 0, 1\right), \tag{8.1}$$

where $\mathcal{F}_{\mathrm{P}}\left(N_j \,|\, \mu \cdot s_j + b_j\right)$ denotes the Poisson distribution with mean $\mu \cdot s_j + b_j$ for variable N_j. The correlations of the systematic uncertainties across categories are taken into account. The expected signal and background event counts in each bin are functions of $\boldsymbol{\theta}$. The parameterisation is chosen such that the rates in each channel are log-normally distributed for a normally distributed $\boldsymbol{\theta}$.

To calculate the upper limit on μ for a given signal hypothesis, the compatibility of the observed or expected dataset with the signal-plus-background prediction is checked following the modified frequentist method known as CL_s [69]. The test statistic $\tilde{q}_\mu$, used in the upper limit derivation, is defined as

$$\tilde{q}_\mu = \begin{cases} -2\ln\left(\dfrac{\mathcal{L}(\mu, \hat{\boldsymbol{\theta}}_\mu)}{\mathcal{L}(0, \hat{\boldsymbol{\theta}}_0)}\right) & \text{if } \hat{\mu} < 0, \\ -2\ln\left(\dfrac{\mathcal{L}(\mu, \hat{\boldsymbol{\theta}}_\mu)}{\mathcal{L}(\hat{\mu}, \hat{\boldsymbol{\theta}})}\right) & \text{if } 0 \leq \hat{\mu} \leq \mu, \\ 0 & \text{if } \hat{\mu} > \mu, \end{cases} \tag{8.2}$$

where $\hat{\mu}$ and $\hat{\boldsymbol{\theta}}$ refer to the global maximum of the likelihood and $\hat{\boldsymbol{\theta}}_\mu$ corresponds to the conditional maximum likelihood for a given μ. The asymptotic approximation [70] is used to evaluate the probability density functions rather than performing pseudo-experiments; the procedure has been validated using ensemble tests.

The significance of an excess in data is quantified with the local p_0-value, the probability that the background processes can produce a fluctuation greater than or equal to the excess observed in data. The test statistic q_0, which is used in the local p_0-value calculation, is defined as:

$$q_0 = \begin{cases} -2\ln\left(\dfrac{\mathcal{L}(0, \hat{\boldsymbol{\theta}}_0)}{\mathcal{L}(\hat{\mu}, \hat{\boldsymbol{\theta}})}\right) & \text{if } \hat{\mu} \geq 0, \\ 0 & \text{if } \hat{\mu} < 0, \end{cases} \tag{8.3}$$

where the notation is the same as in equation 8.2. The equivalent formulation in terms of the number of standard deviations (σ), Z_0, is referred to as the local significance and is defined as:

$$Z_0 = \Phi^{-1}(1 - p_0), \tag{8.4}$$

where Φ^{-1} is the inverse of the cumulative distribution of the Gaussian distribution. The local p_0-value is estimated using the asymptotic approximation for the q_0 distribution [70].

JHEP02(2013)095

9 Results

No significant excess of events above the background-only expectation is observed in the considered channels in 4.7 fb^{-1} to 4.8 fb^{-1} of $\sqrt{s} = 7$ TeV proton-proton collision data. A 95% CL upper limit on $\tan\beta$ is set for each m_A point using the frequentist method described in section 8. This is done using Higgs boson cross-sections calculated in the m_h^{max} scenario with $\mu > 0$ [11]. Results for each of the $\mu\mu$, $\tau_e\tau_\mu$, $\tau_{\text{lep}}\tau_{\text{had}}$ and $\tau_{\text{had}}\tau_{\text{had}}$ final states, as well as for their statistical combination, can be seen in figure 6. The tightest constraint is at $m_A = 130$ GeV, where values of $\tan\beta > 9.3$ are excluded. The expected exclusion for the same point is $\tan\beta > 10.3$. The exclusion of parameter space is significantly increased in comparison to earlier results by the ATLAS Collaboration [7] and complementary to the excluded parameter space from searches at LEP [13]. A significant portion of the MSSM parameter space that is not excluded is still compatible with the assumption that the newly discovered particle at the LHC is one of the neutral CP-even MSSM Higgs bosons [22, 23]. The lowest local p_0-values per channel are 0.014 (2.2σ) at $m_A = 125$ GeV for the $\mu\mu$ channel, 0.014 (2.2σ) at $m_A = 90$ GeV for the $\tau_e\tau_\mu$ channel, 0.067 (1.5σ) at $m_A = 90$ GeV for the $\tau_{\text{lep}}\tau_{\text{had}}$ channel and 0.097 (1.3σ) at $m_A = 140$ GeV for the $\tau_{\text{had}}\tau_{\text{had}}$ channel. The lowest local p_0 for the statistical combination of all channels is 0.004 (2.7σ) at $m_A = 90$ GeV. The significance of this excess is below 2σ, after considering the look-elsewhere effect in the range 90 GeV $\leq m_A \leq$ 500 GeV and $5 \leq \tan\beta \leq 60$ [71].

The outcome of the search is further interpreted in the generic case of a single scalar boson ϕ produced in either the gluon-fusion or b-associated production mode and decaying to $\mu^+\mu^-$ or $\tau^+\tau^-$. Figure 7 shows 95% CL limits based on this interpretation. The exclusion limits for the production cross-section times the branching ratio for a Higgs boson decaying to $\mu^+\mu^-$ or $\tau^+\tau^-$ are shown as a function of the Higgs boson mass.

10 Summary

A search is presented for the neutral Higgs bosons of the Minimal Supersymmetric Standard Model in proton-proton collisions at a centre-of-mass energy of 7 TeV with the ATLAS experiment at the LHC. A significant portion of the available MSSM parameter space is consistent with the assumption that the newly discovered particle at the LHC is one of the neutral CP-even MSSM Higgs bosons. The study is based on a data sample that corresponds to an integrated luminosity of 4.7 fb^{-1} to 4.8 fb^{-1}. The decay modes of the Higgs bosons considered are $h/A/H \to \mu^+\mu^-$, $h/A/H \to \tau_e\tau_\mu$, $h/A/H \to \tau_{\text{lep}}\tau_{\text{had}}$ and $h/A/H \to \tau_{\text{had}}\tau_{\text{had}}$. The analysis selection criteria exploit the two main production mechanisms in the MSSM, the gluon-fusion and b-associated production modes, by introducing categories for event samples with and without an identified b-jet. Since no excess of events over the expected background is observed in the considered channels, 95% CL limits are set in the m_A–$\tan\beta$ plane, excluding a significant fraction of the MSSM parameter space.

Acknowledgments

We thank CERN for the very successful operation of the LHC, as well as the support staff from our institutions without whom ATLAS could not be operated efficiently.

JHEP02(2013)095

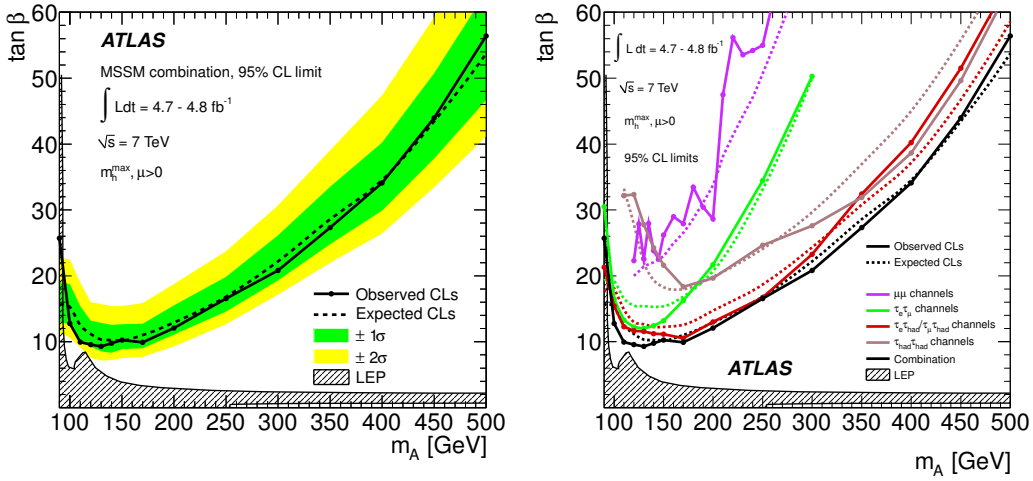

Figure 6. Expected (dashed line) and observed (solid line) 95% CL limits on $\tan\beta$ as a function of m_A for the statistical combination of all channels along with the $\pm 1\,\sigma$ and $\pm 2\,\sigma$ bands for the expected limit are shown on the left plot. Values of $\tan\beta$ greater than the shown lines are excluded. The 95% CL limits for the expected limit (dashed lines) and the observed limit (continuous lines) for each of the $\mu\mu$, $\tau_e\tau_\mu$, $\tau_{\rm lep}\tau_{\rm had}$ and $\tau_{\rm had}\tau_{\rm had}$ channels and their statistical combination are shown on the right plot. The 95% CL exclusion region from neutral MSSM Higgs boson searches performed at LEP [13] is shown in a hatched style.

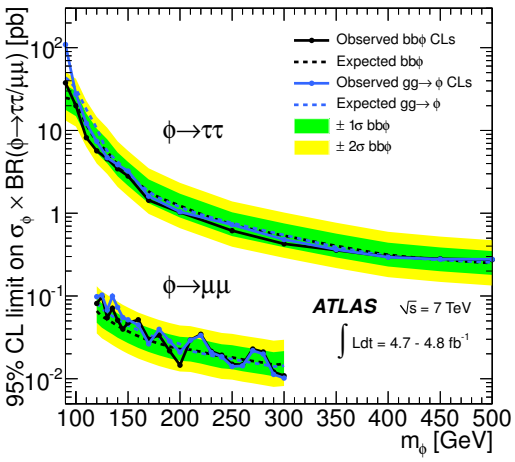

Figure 7. Expected (dashed line) and observed (solid line) 95% CL limits on the cross-section for gluon-fusion and b-associated Higgs boson production times the branching ratio into τ and μ pairs, respectively, along with the $\pm 1\,\sigma$ and $\pm 2\,\sigma$ bands for the expected limit. The combinations of all $\tau\tau$ and $\mu\mu$ channels are shown. The difference in the exclusion limits obtained for the gluon-fusion and the b-associated production modes is due to the different sensitivity from the b-tagged samples.

We acknowledge the support of ANPCyT, Argentina; YerPhI, Armenia; ARC, Australia; BMWF and FWF, Austria; ANAS, Azerbaijan; SSTC, Belarus; CNPq and FAPESP, Brazil; NSERC, NRC and CFI, Canada; CERN; CONICYT, Chile; CAS, MOST and NSFC, China; COLCIENCIAS, Colombia; MSMT CR, MPO CR and VSC CR, Czech Re-

JHEP02(2013)095

public; DNRF, DNSRC and Lundbeck Foundation, Denmark; EPLANET, ERC and NSRF, European Union; IN2P3-CNRS, CEA-DSM/IRFU, France; GNSF, Georgia; BMBF, DFG, HGF, MPG and AvH Foundation, Germany; GSRT and NSRF, Greece; ISF, MINERVA, GIF, DIP and Benoziyo Center, Israel; INFN, Italy; MEXT and JSPS, Japan; CNRST, Morocco; FOM and NWO, Netherlands; BRF and RCN, Norway; MNiSW, Poland; GRICES and FCT, Portugal; MERYS (MECTS), Romania; MES of Russia and ROSATOM, Russian Federation; JINR; MSTD, Serbia; MSSR, Slovakia; ARRS and MVZT, Slovenia; DST/NRF, South Africa; MICINN, Spain; SRC and Wallenberg Foundation, Sweden; SER, SNSF and Cantons of Bern and Geneva, Switzerland; NSC, Taiwan; TAEK, Turkey; STFC, the Royal Society and Leverhulme Trust, United Kingdom; DOE and NSF, United States of America.

The crucial computing support from all WLCG partners is acknowledged gratefully, in particular from CERN and the ATLAS Tier-1 facilities at TRIUMF (Canada), NDGF (Denmark, Norway, Sweden), CC-IN2P3 (France), KIT/GridKA (Germany), INFN-CNAF (Italy), NL-T1 (Netherlands), PIC (Spain), ASGC (Taiwan), RAL (UK) and BNL (USA) and in the Tier-2 facilities worldwide.

References

[1] L. Evans and P. Bryant, *LHC machine*, 2008 *JINST* **3** S08001 [INSPIRE].

[2] F. Englert and R. Brout, *Broken symmetry and the mass of gauge vector mesons*, *Phys. Rev. Lett.* **13** (1964) 321 [INSPIRE].

[3] P.W. Higgs, *Broken symmetries, massless particles and gauge fields*, *Phys. Lett.* **12** (1964) 132 [INSPIRE].

[4] P.W. Higgs, *Broken symmetries and the masses of gauge bosons*, *Phys. Rev. Lett.* **13** (1964) 508 [INSPIRE].

[5] P.W. Higgs, *Spontaneous symmetry breakdown without massless bosons*, *Phys. Rev.* **145** (1966) 1156 [INSPIRE].

[6] G. Guralnik, C. Hagen and T. Kibble, *Global conservation laws and massless particles*, *Phys. Rev. Lett.* **13** (1964) 585 [INSPIRE].

[7] ATLAS collaboration, *Search for neutral MSSM Higgs bosons decaying to $\tau^+\tau^-$ pairs in proton-proton collisions at $\sqrt{s} = 7$ TeV with the ATLAS detector*, *Phys. Lett.* **B 705** (2011) 174 [arXiv:1107.5003] [INSPIRE].

[8] CMS collaboration, *Search for neutral Higgs bosons decaying to τ pairs in pp collisions at $\sqrt{s} = 7$ TeV*, *Phys. Lett.* **B 713** (2012) 68 [arXiv:1202.4083] [INSPIRE].

[9] H.P. Nilles, *Supersymmetry, supergravity and particle physics*, *Phys. Rept.* **110** (1984) 1 [INSPIRE].

[10] H.E. Haber and G.L. Kane, *The search for supersymmetry: probing physics beyond the standard model*, *Phys. Rept.* **117** (1985) 75 [INSPIRE].

JHEP02(2013)095

[11] M.S. Carena, S. Heinemeyer, C. Wagner and G. Weiglein, *Suggestions for benchmark scenarios for MSSM Higgs boson searches at hadron colliders*, *Eur. Phys. J.* **C 26** (2003) 601 [hep-ph/0202167] [INSPIRE].

[12] F. Jegerlehner and A. Nyffeler, *The muon $g-2$*, *Phys. Rept.* **477** (2009) 1 [arXiv:0902.3360] [INSPIRE].

[13] ALEPH, DELPHI, L3, OPAL, LEP Working Group for Higgs Boson Searches collaboration, S. Schael et al., *Search for neutral MSSM Higgs bosons at LEP*, *Eur. Phys. J.* **C 47** (2006) 547 [hep-ex/0602042] [INSPIRE].

[14] Tevatron New Phenomena and Higgs Working Group collaboration, D. Benjamin et al., *Combined CDF and D0 upper limits on MSSM Higgs boson production in τ-τ final states with up to 2.2 fb^{-1}*, arXiv:1003.3363 [INSPIRE].

[15] CDF collaboration, T. Aaltonen et al., *Search for Higgs bosons predicted in two-Higgs-doublet models via decays to τ lepton pairs in 1.96 TeV $p\bar{p}$ collisions*, *Phys. Rev. Lett.* **103** (2009) 201801 [arXiv:0906.1014] [INSPIRE].

[16] D0 collaboration, V. Abazov et al., *Search for Higgs bosons decaying to τ pairs in $p\bar{p}$ collisions with the D0 detector*, *Phys. Rev. Lett.* **101** (2008) 071804 [arXiv:0805.2491] [INSPIRE].

[17] CDF, D0 collaboration, T. Aaltonen et al., *Search for neutral Higgs bosons in events with multiple bottom quarks at the Tevatron*, *Phys. Rev.* **D 86** (2012) 091101 [arXiv:1207.2757] [INSPIRE].

[18] CDF collaboration, T. Aaltonen et al., *Search for Higgs bosons produced in association with b-quarks*, *Phys. Rev.* **D 85** (2012) 032005 [arXiv:1106.4782] [INSPIRE].

[19] D0 collaboration, V.M. Abazov et al., *Search for neutral Higgs bosons in the multi-b-jet topology in 5.2 fb^{-1} of $p\bar{p}$ collisions at $\sqrt{s} = 1.96$ TeV*, *Phys. Lett.* **B 698** (2011) 97 [arXiv:1011.1931] [INSPIRE].

[20] ATLAS collaboration, *Observation of a new particle in the search for the standard model Higgs boson with the ATLAS detector at the LHC*, *Phys. Lett.* **B 716** (2012) 1 [arXiv:1207.7214] [INSPIRE].

[21] CMS collaboration, *Observation of a new boson at a mass of 125 GeV with the CMS experiment at the LHC*, *Phys. Lett.* **B 716** (2012) 30 [arXiv:1207.7235] [INSPIRE].

[22] S. Heinemeyer, O. Stal and G. Weiglein, *Interpreting the LHC Higgs search results in the MSSM*, *Phys. Lett.* **B 710** (2012) 201 [arXiv:1112.3026] [INSPIRE].

[23] A. Arbey, M. Battaglia, A. Djouadi and F. Mahmoudi, *The Higgs sector of the phenomenological MSSM in the light of the Higgs boson discovery*, *JHEP* **09** (2012) 107 [arXiv:1207.1348] [INSPIRE].

[24] ATLAS collaboration, *The ATLAS Experiment at the CERN Large Hadron Collider*, 2008 *JINST* **3** S08003 [INSPIRE].

[25] M. Spira, *HIGLU: a program for the calculation of the total Higgs production cross-section at hadron colliders via gluon fusion including QCD corrections*, hep-ph/9510347 [INSPIRE].

[26] R.V. Harlander and W.B. Kilgore, *Next-to-next-to-leading order Higgs production at hadron colliders*, *Phys. Rev. Lett.* **88** (2002) 201801 [hep-ph/0201206] [INSPIRE].

JHEP02(2013)095

[27] R. Harlander, M. Krämer and M. Schumacher, *Bottom-quark associated Higgs-boson production: reconciling the four- and five-flavour scheme approach*, arXiv:1112.3478 [INSPIRE].

[28] S. Dittmaier, M. Krämer and M. Spira, *Higgs radiation off bottom quarks at the Tevatron and the CERN LHC*, *Phys. Rev.* **D 70** (2004) 074010 [hep-ph/0309204] [INSPIRE].

[29] S. Dawson, C. Jackson, L. Reina and D. Wackeroth, *Exclusive Higgs boson production with bottom quarks at hadron colliders*, *Phys. Rev.* **D 69** (2004) 074027 [hep-ph/0311067] [INSPIRE].

[30] R.V. Harlander and W.B. Kilgore, *Higgs boson production in bottom quark fusion at next-to-next-to leading order*, *Phys. Rev.* **D 68** (2003) 013001 [hep-ph/0304035] [INSPIRE].

[31] M. Frank et al., *The Higgs boson masses and mixings of the complex MSSM in the Feynman-diagrammatic approach*, *JHEP* **02** (2007) 047 [hep-ph/0611326] [INSPIRE].

[32] LHC Higgs Cross Section Working Group collaboration, S. Dittmaier et al., *Handbook of LHC Higgs cross sections: 1. Inclusive observables*, arXiv:1101.0593 [INSPIRE].

[33] S. Alioli, P. Nason, C. Oleari and E. Re, *NLO Higgs boson production via gluon fusion matched with shower in POWHEG*, *JHEP* **04** (2009) 002 [arXiv:0812.0578] [INSPIRE].

[34] T. Gleisberg et al., *Event generation with SHERPA 1.1*, *JHEP* **02** (2009) 007 [arXiv:0811.4622] [INSPIRE].

[35] ATLAS collaboration, *The ATLAS simulation infrastructure*, *Eur. Phys. J.* **C 70** (2010) 823 [arXiv:1005.4568] [INSPIRE].

[36] GEANT4 collaboration, S. Agostinelli et al., *GEANT4: a simulation toolkit*, *Nucl. Instrum. Meth.* **A 506** (2003) 250 [INSPIRE].

[37] M.L. Mangano, M. Moretti, F. Piccinini, R. Pittau and A.D. Polosa, *ALPGEN, a generator for hard multiparton processes in hadronic collisions*, *JHEP* **07** (2003) 001 [hep-ph/0206293] [INSPIRE].

[38] T. Sjöstrand, S. Mrenna and P.Z. Skands, *PYTHIA 6.4 physics and manual*, *JHEP* **05** (2006) 026 [hep-ph/0603175] [INSPIRE].

[39] S. Baranov and M. Smizanska, *Semihard b quark production at high-energies versus data and other approaches*, *Phys. Rev.* **D 62** (2000) 014012 [INSPIRE].

[40] ATLAS collaboration, *Physics analysis tools for beauty physics in ATLAS*, *J. Phys. Conf. Ser.* **119** (2008) 032003 [INSPIRE].

[41] S. Frixione and B.R. Webber, *Matching NLO QCD computations and parton shower simulations*, *JHEP* **06** (2002) 029 [hep-ph/0204244] [INSPIRE].

[42] P. Nason, *A new method for combining NLO QCD with shower Monte Carlo algorithms*, *JHEP* **11** (2004) 040 [hep-ph/0409146] [INSPIRE].

[43] S. Frixione, P. Nason and C. Oleari, *Matching NLO QCD computations with Parton Shower simulations: the POWHEG method*, *JHEP* **11** (2007) 070 [arXiv:0709.2092] [INSPIRE].

[44] B.P. Kersevan and E. Richter-Wąs, *The Monte Carlo event generator AcerMC version 2.0 with interfaces to PYTHIA 6.2 and HERWIG 6.5*, hep-ph/0405247 [INSPIRE].

JHEP02(2013)095

[45] G. Corcella et al., *HERWIG 6: an event generator for hadron emission reactions with interfering gluons (including supersymmetric processes)*, *JHEP* **01** (2001) 010 [hep-ph/0011363] [INSPIRE].

[46] J. Butterworth, J.R. Forshaw and M. Seymour, *Multiparton interactions in photoproduction at HERA*, *Z. Phys.* **C 72** (1996) 637 [hep-ph/9601371] [INSPIRE].

[47] T. Binoth, M. Ciccolini, N. Kauer and M. Krämer, *Gluon-induced W-boson pair production at the LHC*, *JHEP* **12** (2006) 046 [hep-ph/0611170] [INSPIRE].

[48] H.-L. Lai et al., *New parton distributions for collider physics*, *Phys. Rev.* **D 82** (2010) 074024 [arXiv:1007.2241] [INSPIRE].

[49] J. Pumplin et al., *New generation of parton distributions with uncertainties from global QCD analysis*, *JHEP* **07** (2002) 012 [hep-ph/0201195] [INSPIRE].

[50] A. Sherstnev and R. Thorne, *Parton distributions for LO generators*, *Eur. Phys. J.* **C 55** (2008) 553 [arXiv:0711.2473] [INSPIRE].

[51] S. Jadach, J.H. Kuhn and Z. Wąs, *TAUOLA: a library of Monte Carlo programs to simulate decays of polarized τ leptons*, *Comput. Phys. Commun.* **64** (1990) 275 [INSPIRE].

[52] E. Barberio, B. van Eijk and Z. Wąs, *PHOTOS: a universal Monte Carlo for QED radiative corrections in decays*, *Comput. Phys. Commun.* **66** (1991) 115 [INSPIRE].

[53] ATLAS collaboration, *Electron performance measurements with the ATLAS detector using the 2010 LHC proton-proton collision data*, *Eur. Phys. J.* **C 72** (2012) 1909 [arXiv:1110.3174] [INSPIRE].

[54] ATLAS collaboration, *Muon reconstruction efficiency in reprocessed 2010 LHC proton-proton collision data recorded with the ATLAS detector*, ATLAS-CONF-2011-063 (2011).

[55] M. Cacciari, G.P. Salam and G. Soyez, *The anti-k_t jet clustering algorithm*, *JHEP* **04** (2008) 063 [arXiv:0802.1189] [INSPIRE].

[56] W. Lampl et al., *Calorimeter clustering algorithms: description and performance*, ATL-LARG-PUB-2008-002 (2008).

[57] ATLAS collaboration, *Jet energy measurement with the ATLAS detector in proton-proton collisions at $\sqrt{s} = 7$ TeV*, arXiv:1112.6426 [INSPIRE].

[58] ATLAS collaboration, *Measurement of the b-tag efficiency in a sample of jets containing muons with 5 fb^{-1} of data from the ATLAS detector*, ATLAS-CONF-2012-043 (2012).

[59] ATLAS collaboration, *Performance of the reconstruction and identification of hadronic τ decays in ATLAS with 2011 data*, ATLAS-CONF-2012-142 (2012).

[60] ATLAS collaboration, *Performance of missing transverse momentum reconstruction in proton-proton collisions at 7 TeV with ATLAS*, *Eur. Phys. J.* **C 72** (2012) 1844 [arXiv:1108.5602] [INSPIRE].

[61] ATLAS collaboration, *Search for the standard model Higgs boson in the H to $\tau^+\tau^-$ decay mode in $\sqrt{s} = 7$ TeV pp collisions with ATLAS*, *JHEP* **09** (2012) 070 [arXiv:1206.5971] [INSPIRE].

[62] ATLAS collaboration, *Measurement of the $Z \to \tau\tau$ cross section with the ATLAS detector*, *Phys. Rev.* **D 84** (2011) 112006 [arXiv:1108.2016] [INSPIRE].

JHEP02(2013)095

[63] A. Elagin, P. Murat, A. Pranko and A. Safonov, *A new mass reconstruction technique for resonances decaying to di-τ*, *Nucl. Instrum. Meth.* **A 654** (2011) 481 [arXiv:1012.4686] [INSPIRE].

[64] R. Hamberg, W. van Neerven and T. Matsuura, *A complete calculation of the order α_s^2 correction to the Drell-Yan K factor*, *Nucl. Phys.* **B 359** (1991) 343 [*Erratum ibid.* **B 644** (2002) 403-404] [INSPIRE].

[65] C. Anastasiou, L.J. Dixon, K. Melnikov and F. Petriello, *High precision QCD at hadron colliders: electroweak gauge boson rapidity distributions at NNLO*, *Phys. Rev.* **D 69** (2004) 094008 [hep-ph/0312266] [INSPIRE].

[66] ATLAS collaboration, *Measurement of the mistag rate with 5 fb^{-1} of data collected by the ATLAS detector*, ATLAS-CONF-2012-040 (2012).

[67] ATLAS collaboration, *Luminosity determination in pp collisions at $\sqrt{s} = 7$ TeV using the ATLAS detector in 2011*, ATLAS-CONF-2011-116 (2011).

[68] ATLAS collaboration, *Luminosity determination in pp collisions at $\sqrt{s} = 7$ TeV using the ATLAS detector at the LHC*, *Eur. Phys. J.* **C 71** (2011) 1630 [arXiv:1101.2185] [INSPIRE].

[69] A.L. Read, *Presentation of search results: the CL_s technique*, *J. Phys.* **G 28** (2002) 2693 [INSPIRE].

[70] G. Cowan, K. Cranmer, E. Gross and O. Vitells, *Asymptotic formulae for likelihood-based tests of new physics*, *Eur. Phys. J.* **C 71** (2011) 1554 [arXiv:1007.1727] [INSPIRE].

[71] O. Vitells and E. Gross, *Estimating the significance of a signal in a multi-dimensional search*, *Astropart. Phys.* **35** (2011) 230 [arXiv:1105.4355] [INSPIRE].

JHEP02(2013)095

The ATLAS collaboration

G. Aad[48], T. Abajyan[21], B. Abbott[111], J. Abdallah[12], S. Abdel Khalek[115], A.A. Abdelalim[49], O. Abdinov[11], R. Aben[105], B. Abi[112], M. Abolins[88], O.S. AbouZeid[158], H. Abramowicz[153], H. Abreu[136], B.S. Acharya[164a,164b,a], L. Adamczyk[38], D.L. Adams[25], T.N. Addy[56], J. Adelman[176], S. Adomeit[98], P. Adragna[75], T. Adye[129], S. Aefsky[23], J.A. Aguilar-Saavedra[124b,b], M. Agustoni[17], S.P. Ahlen[22], F. Ahles[48], A. Ahmad[148], M. Ahsan[41], G. Aielli[133a,133b], T.P.A. Åkesson[79], G. Akimoto[155], A.V. Akimov[94], M.A. Alam[76], J. Albert[169], S. Albrand[55], M. Aleksa[30], I.N. Aleksandrov[64], F. Alessandria[89a], C. Alexa[26a], G. Alexander[153], G. Alexandre[49], T. Alexopoulos[10], M. Alhroob[164a,164c], M. Aliev[16], G. Alimonti[89a], J. Alison[120], B.M.M. Allbrooke[18], L.J. Allison[71], P.P. Allport[73], S.E. Allwood-Spiers[53], J. Almond[82], A. Aloisio[102a,102b], R. Alon[172], A. Alonso[79], F. Alonso[70], A. Altheimer[35], B. Alvarez Gonzalez[88], M.G. Alviggi[102a,102b], K. Amako[65], C. Amelung[23], V.V. Ammosov[128,*], S.P. Amor Dos Santos[124a], A. Amorim[124a,c], S. Amoroso[48], N. Amram[153], C. Anastopoulos[30], L.S. Ancu[17], N. Andari[115], T. Andeen[35], C.F. Anders[58b], G. Anders[58a], K.J. Anderson[31], A. Andreazza[89a,89b], V. Andrei[58a], M-L. Andrieux[55], X.S. Anduaga[70], S. Angelidakis[9], P. Anger[44], A. Angerami[35], F. Anghinolfi[30], A. Anisenkov[107], N. Anjos[124a], A. Annovi[47], A. Antonaki[9], M. Antonelli[47], A. Antonov[96], J. Antos[144b], F. Anulli[132a], M. Aoki[101], S. Aoun[83], L. Aperio Bella[5], R. Apolle[118,d], G. Arabidze[88], I. Aracena[143], Y. Arai[65], A.T.H. Arce[45], S. Arfaoui[148], J-F. Arguin[93], S. Argyropoulos[42], E. Arik[19a,*], M. Arik[19a], A.J. Armbruster[87], O. Arnaez[81], V. Arnal[80], A. Artamonov[95], G. Artoni[132a,132b], D. Arutinov[21], S. Asai[155], S. Ask[28], B. Åsman[146a,146b], L. Asquith[6], K. Assamagan[25,e], A. Astbury[169], M. Atkinson[165], B. Aubert[5], E. Auge[115], K. Augsten[126], M. Aurousseau[145a], G. Avolio[30], D. Axen[168], G. Azuelos[93,f], Y. Azuma[155], M.A. Baak[30], G. Baccaglioni[89a], C. Bacci[134a,134b], A.M. Bach[15], H. Bachacou[136], K. Bachas[154], M. Backes[49], M. Backhaus[21], J. Backus Mayes[143], E. Badescu[26a], P. Bagnaia[132a,132b], Y. Bai[33a], D.C. Bailey[158], T. Bain[35], J.T. Baines[129], O.K. Baker[176], S. Baker[77], P. Balek[127], E. Banas[39], P. Banerjee[93], Sw. Banerjee[173], D. Banfi[30], A. Bangert[150], V. Bansal[169], H.S. Bansil[18], L. Barak[172], S.P. Baranov[94], T. Barber[48], E.L. Barberio[86], D. Barberis[50a,50b], M. Barbero[21], D.Y. Bardin[64], T. Barillari[99], M. Barisonzi[175], T. Barklow[143], N. Barlow[28], B.M. Barnett[129], R.M. Barnett[15], A. Baroncelli[134a], G. Barone[49], A.J. Barr[118], F. Barreiro[80], J. Barreiro Guimarães da Costa[57], R. Bartoldus[143], A.E. Barton[71], V. Bartsch[149], A. Basye[165], R.L. Bates[53], L. Batkova[144a], J.R. Batley[28], A. Battaglia[17], M. Battistin[30], F. Bauer[136], H.S. Bawa[143,g], S. Beale[98], T. Beau[78], P.H. Beauchemin[161], R. Beccherle[50a], P. Bechtle[21], H.P. Beck[17], K. Becker[175], S. Becker[98], M. Beckingham[138], K.H. Becks[175], A.J. Beddall[19c], A. Beddall[19c], S. Bedikian[176], V.A. Bednyakov[64], C.P. Bee[83], L.J. Beemster[105], M. Begel[25], S. Behar Harpaz[152], P.K. Behera[62], M. Beimforde[99], C. Belanger-Champagne[85], P.J. Bell[49], W.H. Bell[49], G. Bella[153], L. Bellagamba[20a], M. Bellomo[30], A. Belloni[57], O. Beloborodova[107,h], K. Belotskiy[96], O. Beltramello[30], O. Benary[153], D. Benchekroun[135a], K. Bendtz[146a,146b], N. Benekos[165], Y. Benhammou[153], E. Benhar Noccioli[49], J.A. Benitez Garcia[159b], D.P. Benjamin[45], M. Benoit[115], J.R. Bensinger[23], K. Benslama[130], S. Bentvelsen[105], D. Berge[30], E. Bergeaas Kuutmann[42], N. Berger[5], F. Berghaus[169], E. Berglund[105], J. Beringer[15], P. Bernat[77], R. Bernhard[48], C. Bernius[25], T. Berry[76], C. Bertella[83], A. Bertin[20a,20b], F. Bertolucci[122a,122b], M.I. Besana[89a,89b], G.J. Besjes[104], N. Besson[136], S. Bethke[99], W. Bhimji[46], R.M. Bianchi[30], L. Bianchini[23], M. Bianco[72a,72b], O. Biebel[98], S.P. Bieniek[77], K. Bierwagen[54], J. Biesiada[15], M. Biglietti[134a], H. Bilokon[47], M. Bindi[20a,20b], S. Binet[115], A. Bingul[19c], C. Bini[132a,132b], C. Biscarat[178], B. Bittner[99], C.W. Black[150], K.M. Black[22], R.E. Blair[6], J.-B. Blanchard[136], T. Blazek[144a], I. Bloch[42], C. Blocker[23], J. Blocki[39], W. Blum[81], U. Blumenschein[54], G.J. Bobbink[105], V.S. Bobrovnikov[107], S.S. Bocchetta[79], A. Bocci[45], C.R. Boddy[118], M. Boehler[48],

JHEP02(2013)095

J. Boek[175], T.T. Boek[175], N. Boelaert[36], J.A. Bogaerts[30], A. Bogdanchikov[107], A. Bogouch[90,*], C. Bohm[146a], J. Bohm[125], V. Boisvert[76], T. Bold[38], V. Boldea[26a], N.M. Bolnet[136], M. Bomben[78], M. Bona[75], M. Boonekamp[136], S. Bordoni[78], C. Borer[17], A. Borisov[128], G. Borissov[71], I. Borjanovic[13a], M. Borri[82], S. Borroni[42], J. Bortfeldt[98], V. Bortolotto[134a,134b], K. Bos[105], D. Boscherini[20a], M. Bosman[12], H. Boterenbrood[105], J. Bouchami[93], J. Boudreau[123], E.V. Bouhova-Thacker[71], D. Boumediene[34], C. Bourdarios[115], N. Bousson[83], A. Boveia[31], J. Boyd[30], I.R. Boyko[64], I. Bozovic-Jelisavcic[13b], J. Bracinik[18], P. Branchini[134a], A. Brandt[8], G. Brandt[118], O. Brandt[54], U. Bratzler[156], B. Brau[84], J.E. Brau[114], H.M. Braun[175,*], S.F. Brazzale[164a,164c], B. Brelier[158], J. Bremer[30], K. Brendlinger[120], R. Brenner[166], S. Bressler[172], T.M. Bristow[145b], D. Britton[53], F.M. Brochu[28], I. Brock[21], R. Brock[88], F. Broggi[89a], C. Bromberg[88], J. Bronner[99], G. Brooijmans[35], T. Brooks[76], W.K. Brooks[32b], G. Brown[82], P.A. Bruckman de Renstrom[39], D. Bruncko[144b], R. Bruneliere[48], S. Brunet[60], A. Bruni[20a], G. Bruni[20a], M. Bruschi[20a], L. Bryngemark[79], T. Buanes[14], Q. Buat[55], F. Bucci[49], J. Buchanan[118], P. Buchholz[141], R.M. Buckingham[118], A.G. Buckley[46], S.I. Buda[26a], I.A. Budagov[64], B. Budick[108], V. Büscher[81], L. Bugge[117], O. Bulekov[96], A.C. Bundock[73], M. Bunse[43], T. Buran[117], H. Burckhart[30], S. Burdin[73], T. Burgess[14], S. Burke[129], E. Busato[34], P. Bussey[53], C.P. Buszello[166], B. Butler[143], J.M. Butler[22], C.M. Buttar[53], J.M. Butterworth[77], W. Buttinger[28], M. Byszewski[30], S. Cabrera Urbán[167], D. Caforio[20a,20b], O. Cakir[4a], P. Calafiura[15], G. Calderini[78], P. Calfayan[98], R. Calkins[106], L.P. Caloba[24a], R. Caloi[132a,132b], D. Calvet[34], S. Calvet[34], R. Camacho Toro[34], P. Camarri[133a,133b], D. Cameron[117], L.M. Caminada[15], R. Caminal Armadans[12], S. Campana[30], M. Campanelli[77], V. Canale[102a,102b], F. Canelli[31], A. Canepa[159a], J. Cantero[80], R. Cantrill[76], M.D.M. Capeans Garrido[30], I. Caprini[26a], M. Caprini[26a], D. Capriotti[99], M. Capua[37a,37b], R. Caputo[81], R. Cardarelli[133a], T. Carli[30], G. Carlino[102a], L. Carminati[89a,89b], S. Caron[104], E. Carquin[32b], G.D. Carrillo-Montoya[145b], A.A. Carter[75], J.R. Carter[28], J. Carvalho[124a,i], D. Casadei[108], M.P. Casado[12], M. Cascella[122a,122b], C. Caso[50a,50b,*], A.M. Castaneda Hernandez[173,j], E. Castaneda-Miranda[173], V. Castillo Gimenez[167], N.F. Castro[124a], G. Cataldi[72a], P. Catastini[57], A. Catinaccio[30], J.R. Catmore[30], A. Cattai[30], G. Cattani[133a,133b], S. Caughron[88], V. Cavaliere[165], P. Cavalleri[78], D. Cavalli[89a], M. Cavalli-Sforza[12], V. Cavasinni[122a,122b], F. Ceradini[134a,134b], A.S. Cerqueira[24b], A. Cerri[15], L. Cerrito[75], F. Cerutti[15], S.A. Cetin[19b], A. Chafaq[135a], D. Chakraborty[106], I. Chalupkova[127], K. Chan[3], P. Chang[165], B. Chapleau[85], J.D. Chapman[28], J.W. Chapman[87], D.G. Charlton[18], V. Chavda[82], C.A. Chavez Barajas[30], S. Cheatham[85], S. Chekanov[6], S.V. Chekulaev[159a], G.A. Chelkov[64], M.A. Chelstowska[104], C. Chen[63], H. Chen[25], S. Chen[33c], X. Chen[173], Y. Chen[35], Y. Cheng[31], A. Cheplakov[64], R. Cherkaoui El Moursli[135e], V. Chernyatin[25], E. Cheu[7], S.L. Cheung[158], L. Chevalier[136], G. Chiefari[102a,102b], L. Chikovani[51a,*], J.T. Childers[30], A. Chilingarov[71], G. Chiodini[72a], A.S. Chisholm[18], R.T. Chislett[77], A. Chitan[26a], M.V. Chizhov[64], G. Choudalakis[31], S. Chouridou[137], I.A. Christidi[77], A. Christov[48], D. Chromek-Burckhart[30], M.L. Chu[151], J. Chudoba[125], G. Ciapetti[132a,132b], A.K. Ciftci[4a], R. Ciftci[4a], D. Cinca[34], V. Cindro[74], A. Ciocio[15], M. Cirilli[87], P. Cirkovic[13b], Z.H. Citron[172], M. Citterio[89a], M. Ciubancan[26a], A. Clark[49], P.J. Clark[46], R.N. Clarke[15], W. Cleland[123], J.C. Clemens[83], B. Clement[55], C. Clement[146a,146b], Y. Coadou[83], M. Cobal[164a,164c], A. Coccaro[138], J. Cochran[63], L. Coffey[23], J.G. Cogan[143], J. Coggeshall[165], J. Colas[5], S. Cole[106], A.P. Colijn[105], N.J. Collins[18], C. Collins-Tooth[53], J. Collot[55], T. Colombo[119a,119b], G. Colon[84], G. Compostella[99], P. Conde Muiño[124a], E. Coniavitis[166], M.C. Conidi[12], S.M. Consonni[89a,89b], V. Consorti[48], S. Constantinescu[26a], C. Conta[119a,119b], G. Conti[57], F. Conventi[102a,k], M. Cooke[15], B.D. Cooper[77], A.M. Cooper-Sarkar[118], K. Copic[15], T. Cornelissen[175], M. Corradi[20a], F. Corriveau[85,l], A. Cortes-Gonzalez[165], G. Cortiana[99],

JHEP02(2013)095

G. Costa[89a], M.J. Costa[167], D. Costanzo[139], D. Côté[30], L. Courneyea[169], G. Cowan[76], B.E. Cox[82], K. Cranmer[108], F. Crescioli[78], M. Cristinziani[21], G. Crosetti[37a,37b], S. Crépé-Renaudin[55], C.-M. Cuciuc[26a], C. Cuenca Almenar[176], T. Cuhadar Donszelmann[139], J. Cummings[176], M. Curatolo[47], C.J. Curtis[18], C. Cuthbert[150], P. Cwetanski[60], H. Czirr[141], P. Czodrowski[44], Z. Czyczula[176], S. D'Auria[53], M. D'Onofrio[73], A. D'Orazio[132a,132b], M.J. Da Cunha Sargedas De Sousa[124a], C. Da Via[82], W. Dabrowski[38], A. Dafinca[118], T. Dai[87], F. Dallaire[93], C. Dallapiccola[84], M. Dam[36], M. Dameri[50a,50b], D.S. Damiani[137], H.O. Danielsson[30], V. Dao[104], G. Darbo[50a], G.L. Darlea[26b], J.A. Dassoulas[42], W. Davey[21], T. Davidek[127], N. Davidson[86], R. Davidson[71], E. Davies[118,d], M. Davies[93], O. Davignon[78], A.R. Davison[77], Y. Davygora[58a], E. Dawe[142], I. Dawson[139], R.K. Daya-Ishmukhametova[23], K. De[8], R. de Asmundis[102a], S. De Castro[20a,20b], S. De Cecco[78], J. de Graat[98], N. De Groot[104], P. de Jong[105], C. De La Taille[115], H. De la Torre[80], F. De Lorenzi[63], L. De Nooij[105], D. De Pedis[132a], A. De Salvo[132a], U. De Sanctis[164a,164c], A. De Santo[149], J.B. De Vivie De Regie[115], G. De Zorzi[132a,132b], W.J. Dearnaley[71], R. Debbe[25], C. Debenedetti[46], B. Dechenaux[55], D.V. Dedovich[64], J. Degenhardt[120], J. Del Peso[80], T. Del Prete[122a,122b], T. Delemontex[55], M. Deliyergiyev[74], A. Dell'Acqua[30], L. Dell'Asta[22], M. Della Pietra[102a,k], D. della Volpe[102a,102b], M. Delmastro[5], P.A. Delsart[55], C. Deluca[105], S. Demers[176], M. Demichev[64], B. Demirkoz[12,m], S.P. Denisov[128], D. Derendarz[39], J.E. Derkaoui[135d], F. Derue[78], P. Dervan[73], K. Desch[21], E. Devetak[148], P.O. Deviveiros[105], A. Dewhurst[129], B. DeWilde[148], S. Dhaliwal[158], R. Dhullipudi[25,n], A. Di Ciaccio[133a,133b], L. Di Ciaccio[5], C. Di Donato[102a,102b], A. Di Girolamo[30], B. Di Girolamo[30], S. Di Luise[134a,134b], A. Di Mattia[152], B. Di Micco[30], R. Di Nardo[47], A. Di Simone[133a,133b], R. Di Sipio[20a,20b], M.A. Diaz[32a], E.B. Diehl[87], J. Dietrich[42], T.A. Dietzsch[58a], S. Diglio[86], K. Dindar Yagci[40], J. Dingfelder[21], F. Dinut[26a], C. Dionisi[132a,132b], P. Dita[26a], S. Dita[26a], F. Dittus[30], F. Djama[83], T. Djobava[51b], M.A.B. do Vale[24c], A. Do Valle Wemans[124a,o], T.K.O. Doan[5], M. Dobbs[85], D. Dobos[30], E. Dobson[30,p], J. Dodd[35], C. Doglioni[49], T. Doherty[53], Y. Doi[65,*], J. Dolejsi[127], Z. Dolezal[127], B.A. Dolgoshein[96,*], T. Dohmae[155], M. Donadelli[24d], J. Donini[34], J. Dopke[30], A. Doria[102a], A. Dos Anjos[173], A. Dotti[122a,122b], M.T. Dova[70], A.D. Doxiadis[105], A.T. Doyle[53], N. Dressnandt[120], M. Dris[10], J. Dubbert[99], S. Dube[15], E. Dubreuil[34], E. Duchovni[172], G. Duckeck[98], D. Duda[175], A. Dudarev[30], F. Dudziak[63], M. Dührssen[30], I.P. Duerdoth[82], L. Duflot[115], M-A. Dufour[85], L. Duguid[76], M. Dunford[58a], H. Duran Yildiz[4a], R. Duxfield[139], M. Dwuznik[38], M. Düren[52], W.L. Ebenstein[45], J. Ebke[98], S. Eckweiler[81], W. Edson[2], C.A. Edwards[76], N.C. Edwards[53], W. Ehrenfeld[21], T. Eifert[143], G. Eigen[14], K. Einsweiler[15], E. Eisenhandler[75], T. Ekelof[166], M. El Kacimi[135c], M. Ellert[166], S. Elles[5], F. Ellinghaus[81], K. Ellis[75], N. Ellis[30], J. Elmsheuser[98], M. Elsing[30], D. Emeliyanov[129], R. Engelmann[148], A. Engl[98], B. Epp[61], J. Erdmann[176], A. Ereditato[17], D. Eriksson[146a], J. Ernst[2], M. Ernst[25], J. Ernwein[136], D. Errede[165], S. Errede[165], E. Ertel[81], M. Escalier[115], H. Esch[43], C. Escobar[123], X. Espinal Curull[12], B. Esposito[47], F. Etienne[83], A.I. Etienvre[136], E. Etzion[153], D. Evangelakou[54], H. Evans[60], L. Fabbri[20a,20b], C. Fabre[30], R.M. Fakhrutdinov[128], S. Falciano[132a], Y. Fang[33a], M. Fanti[89a,89b], A. Farbin[8], A. Farilla[134a], J. Farley[148], T. Farooque[158], S. Farrell[163], S.M. Farrington[170], P. Farthouat[30], F. Fassi[167], P. Fassnacht[30], D. Fassouliotis[9], B. Fatholahzadeh[158], A. Favareto[89a,89b], L. Fayard[115], P. Federic[144a], O.L. Fedin[121], W. Fedorko[168], M. Fehling-Kaschek[48], L. Feligioni[83], C. Feng[33d], E.J. Feng[6], A.B. Fenyuk[128], J. Ferencei[144b], W. Fernando[6], S. Ferrag[53], J. Ferrando[53], V. Ferrara[42], A. Ferrari[166], P. Ferrari[105], R. Ferrari[119a], D.E. Ferreira de Lima[53], A. Ferrer[167], D. Ferrere[49], C. Ferretti[87], A. Ferretto Parodi[50a,50b], M. Fiascaris[31], F. Fiedler[81], A. Filipčič[74], F. Filthaut[104], M. Fincke-Keeler[169], M.C.N. Fiolhais[124a,i], L. Fiorini[167], A. Firan[40], G. Fischer[42], M.J. Fisher[109], E.A. Fitzgerald[23], M. Flechl[48], I. Fleck[141], J. Fleckner[81],

JHEP02(2013)095

P. Fleischmann[174], S. Fleischmann[175], G. Fletcher[75], T. Flick[175], A. Floderus[79], L.R. Flores Castillo[173], A.C. Florez Bustos[159b], M.J. Flowerdew[99], T. Fonseca Martin[17], A. Formica[136], A. Forti[82], D. Fortin[159a], D. Fournier[115], A.J. Fowler[45], H. Fox[71], P. Francavilla[12], M. Franchini[20a,20b], S. Franchino[119a,119b], D. Francis[30], T. Frank[172], M. Franklin[57], S. Franz[30], M. Fraternali[119a,119b], S. Fratina[120], S.T. French[28], C. Friedrich[42], F. Friedrich[44], D. Froidevaux[30], J.A. Frost[28], C. Fukunaga[156], E. Fullana Torregrosa[127], B.G. Fulsom[143], J. Fuster[167], C. Gabaldon[30], O. Gabizon[172], T. Gadfort[25], S. Gadomski[49], G. Gagliardi[50a,50b], P. Gagnon[60], C. Galea[98], B. Galhardo[124a], E.J. Gallas[118], V. Gallo[17], B.J. Gallop[129], P. Gallus[126], K.K. Gan[109], Y.S. Gao[143,g], A. Gaponenko[15], F. Garberson[176], M. Garcia-Sciveres[15], C. García[167], J.E. García Navarro[167], R.W. Gardner[31], N. Garelli[143], V. Garonne[30], C. Gatti[47], G. Gaudio[119a], B. Gaur[141], L. Gauthier[136], P. Gauzzi[132a,132b], I.L. Gavrilenko[94], C. Gay[168], G. Gaycken[21], E.N. Gazis[10], P. Ge[33d], Z. Gecse[168], C.N.P. Gee[129], D.A.A. Geerts[105], Ch. Geich-Gimbel[21], K. Gellerstedt[146a,146b], C. Gemme[50a], A. Gemmell[53], M.H. Genest[55], S. Gentile[132a,132b], M. George[54], S. George[76], D. Gerbaudo[12], P. Gerlach[175], A. Gershon[153], C. Geweniger[58a], H. Ghazlane[135b], N. Ghodbane[34], B. Giacobbe[20a], S. Giagu[132a,132b], V. Giangiobbe[12], F. Gianotti[30], B. Gibbard[25], A. Gibson[158], S.M. Gibson[30], M. Gilchriese[15], D. Gillberg[30], A.R. Gillman[129], D.M. Gingrich[3,f], J. Ginzburg[153], N. Giokaris[9], M.P. Giordani[164c], R. Giordano[102a,102b], F.M. Giorgi[16], P. Giovannini[99], P.F. Giraud[136], D. Giugni[89a], M. Giunta[93], B.K. Gjelsten[117], L.K. Gladilin[97], C. Glasman[80], J. Glatzer[21], A. Glazov[42], G.L. Glonti[64], J.R. Goddard[75], J. Godfrey[142], J. Godlewski[30], M. Goebel[42], T. Göpfert[44], C. Goeringer[81], C. Gössling[43], S. Goldfarb[87], T. Golling[176], D. Golubkov[128], A. Gomes[124a,c], L.S. Gomez Fajardo[42], R. Gonçalo[76], J. Goncalves Pinto Firmino Da Costa[42], L. Gonella[21], S. González de la Hoz[167], G. Gonzalez Parra[12], M.L. Gonzalez Silva[27], S. Gonzalez-Sevilla[49], J.J. Goodson[148], L. Goossens[30], P.A. Gorbounov[95], H.A. Gordon[25], I. Gorelov[103], G. Gorfine[175], B. Gorini[30], E. Gorini[72a,72b], A. Gorišek[74], E. Gornicki[39], A.T. Goshaw[6], M. Gosselink[105], M.I. Gostkin[64], I. Gough Eschrich[163], M. Gouighri[135a], D. Goujdami[135c], M.P. Goulette[49], A.G. Goussiou[138], C. Goy[5], S. Gozpinar[23], I. Grabowska-Bold[38], P. Grafström[20a,20b], K-J. Grahn[42], E. Gramstad[117], F. Grancagnolo[72a], S. Grancagnolo[16], V. Grassi[148], V. Gratchev[121], H.M. Gray[30], J.A. Gray[148], E. Graziani[134a], O.G. Grebenyuk[121], T. Greenshaw[73], Z.D. Greenwood[25,n], K. Gregersen[36], I.M. Gregor[42], P. Grenier[143], J. Griffiths[8], N. Grigalashvili[64], A.A. Grillo[137], K. Grimm[71], S. Grinstein[12], Ph. Gris[34], Y.V. Grishkevich[97], J.-F. Grivaz[115], A. Grohsjean[42], E. Gross[172], J. Grosse-Knetter[54], J. Groth-Jensen[172], K. Grybel[141], D. Guest[176], C. Guicheney[34], E. Guido[50a,50b], T. Guillemin[115], S. Guindon[54], U. Gul[53], J. Gunther[125], B. Guo[158], J. Guo[35], P. Gutierrez[111], N. Guttman[153], O. Gutzwiller[173], C. Guyot[136], C. Gwenlan[118], C.B. Gwilliam[73], A. Haas[108], S. Haas[30], C. Haber[15], H.K. Hadavand[8], D.R. Hadley[18], P. Haefner[21], F. Hahn[30], Z. Hajduk[39], H. Hakobyan[177], D. Hall[118], G. Halladjian[62], K. Hamacher[175], P. Hamal[113], K. Hamano[86], M. Hamer[54], A. Hamilton[145b,q], S. Hamilton[161], L. Han[33b], K. Hanagaki[116], K. Hanawa[160], M. Hance[15], C. Handel[81], P. Hanke[58a], J.R. Hansen[36], J.B. Hansen[36], J.D. Hansen[36], P.H. Hansen[36], P. Hansson[143], K. Hara[160], T. Harenberg[175], S. Harkusha[90], D. Harper[87], R.D. Harrington[46], O.M. Harris[138], J. Hartert[48], F. Hartjes[105], T. Haruyama[65], A. Harvey[56], S. Hasegawa[101], Y. Hasegawa[140], S. Hassani[136], S. Haug[17], M. Hauschild[30], R. Hauser[88], M. Havranek[21], C.M. Hawkes[18], R.J. Hawkings[30], A.D. Hawkins[79], T. Hayakawa[66], T. Hayashi[160], D. Hayden[76], C.P. Hays[118], H.S. Hayward[73], S.J. Haywood[129], S.J. Head[18], V. Hedberg[79], L. Heelan[8], S. Heim[120], B. Heinemann[15], S. Heisterkamp[36], L. Helary[22], C. Heller[98], M. Heller[30], S. Hellman[146a,146b], D. Hellmich[21], C. Helsens[12], R.C.W. Henderson[71], M. Henke[58a], A. Henrichs[176], A.M. Henriques Correia[30], S. Henrot-Versille[115], C. Hensel[54], C.M. Hernandez[8], Y. Hernández Jiménez[167], R. Herrberg[16], G. Herten[48],

JHEP02(2013)095

R. Hertenberger[98], L. Hervas[30], G.G. Hesketh[77], N.P. Hessey[105], R. Hickling[75], E. Higón-Rodriguez[167], J.C. Hill[28], K.H. Hiller[42], S. Hillert[21], S.J. Hillier[18], I. Hinchliffe[15], E. Hines[120], M. Hirose[116], F. Hirsch[43], D. Hirschbuehl[175], J. Hobbs[148], N. Hod[153], M.C. Hodgkinson[139], P. Hodgson[139], A. Hoecker[30], M.R. Hoeferkamp[103], J. Hoffman[40], D. Hoffmann[83], M. Hohlfeld[81], M. Holder[141], S.O. Holmgren[146a], T. Holy[126], J.L. Holzbauer[88], T.M. Hong[120], L. Hooft van Huysduynen[108], S. Horner[48], J-Y. Hostachy[55], S. Hou[151], A. Hoummada[135a], J. Howard[118], J. Howarth[82], I. Hristova[16], J. Hrivnac[115], T. Hryn'ova[5], P.J. Hsu[81], S.-C. Hsu[138], D. Hu[35], Z. Hubacek[30], F. Hubaut[83], F. Huegging[21], A. Huettmann[42], T.B. Huffman[118], E.W. Hughes[35], G. Hughes[71], M. Huhtinen[30], M. Hurwitz[15], N. Huseynov[64,r], J. Huston[88], J. Huth[57], G. Iacobucci[49], G. Iakovidis[10], M. Ibbotson[82], I. Ibragimov[141], L. Iconomidou-Fayard[115], J. Idarraga[115], P. Iengo[102a], O. Igonkina[105], Y. Ikegami[65], M. Ikeno[65], D. Iliadis[154], N. Ilic[158], T. Ince[99], P. Ioannou[9], M. Iodice[134a], K. Iordanidou[9], V. Ippolito[132a,132b], A. Irles Quiles[167], C. Isaksson[166], M. Ishino[67], M. Ishitsuka[157], R. Ishmukhametov[109], C. Issever[118], S. Istin[19a], A.V. Ivashin[128], W. Iwanski[39], H. Iwasaki[65], J.M. Izen[41], V. Izzo[102a], B. Jackson[120], J.N. Jackson[73], P. Jackson[1], M.R. Jaekel[30], V. Jain[2], K. Jakobs[48], S. Jakobsen[36], T. Jakoubek[125], J. Jakubek[126], D.O. Jamin[151], D.K. Jana[111], E. Jansen[77], H. Jansen[30], J. Janssen[21], A. Jantsch[99], M. Janus[48], R.C. Jared[173], G. Jarlskog[79], L. Jeanty[57], I. Jen-La Plante[31], G.-Y. Jeng[150], D. Jennens[86], P. Jenni[30], A.E. Loevschall-Jensen[36], P. Ježˇ[36], S. Jézéquel[5], M.K. Jha[20a], H. Ji[173], W. Ji[81], J. Jia[148], Y. Jiang[33b], M. Jimenez Belenguer[42], S. Jin[33a], O. Jinnouchi[157], M.D. Joergensen[36], D. Joffe[40], M. Johansen[146a,146b], K.E. Johansson[146a], P. Johansson[139], S. Johnert[42], K.A. Johns[7], K. Jon-And[146a,146b], G. Jones[170], R.W.L. Jones[71], T.J. Jones[73], C. Joram[30], P.M. Jorge[124a], K.D. Joshi[82], J. Jovicevic[147], T. Jovin[13b], X. Ju[173], C.A. Jung[43], R.M. Jungst[30], V. Juranek[125], P. Jussel[61], A. Juste Rozas[12], S. Kabana[17], M. Kaci[167], A. Kaczmarska[39], P. Kadlecik[36], M. Kado[115], H. Kagan[109], M. Kagan[57], E. Kajomovitz[152], S. Kalinin[175], L.V. Kalinovskaya[64], S. Kama[40], N. Kanaya[155], M. Kaneda[30], S. Kaneti[28], T. Kanno[157], V.A. Kantserov[96], J. Kanzaki[65], B. Kaplan[108], A. Kapliy[31], D. Kar[53], M. Karagounis[21], K. Karakostas[10], M. Karnevskiy[58b], V. Kartvelishvili[71], A.N. Karyukhin[128], L. Kashif[173], G. Kasieczka[58b], R.D. Kass[109], A. Kastanas[14], M. Kataoka[5], Y. Kataoka[155], J. Katzy[42], V. Kaushik[7], K. Kawagoe[69], T. Kawamoto[155], G. Kawamura[81], S. Kazama[155], V.F. Kazanin[107], M.Y. Kazarinov[64], R. Keeler[169], P.T. Keener[120], R. Kehoe[40], M. Keil[54], G.D. Kekelidze[64], J.S. Keller[138], M. Kenyon[53], H. Keoshkerian[5], O. Kepka[125], N. Kerschen[30], B.P. Kerševan[74], S. Kersten[175], K. Kessoku[155], J. Keung[158], F. Khalil-zada[11], H. Khandanyan[146a,146b], A. Khanov[112], D. Kharchenko[64], A. Khodinov[96], A. Khomich[58a], T.J. Khoo[28], G. Khoriauli[21], A. Khoroshilov[175], V. Khovanskiy[95], E. Khramov[64], J. Khubua[51b], H. Kim[146a,146b], S.H. Kim[160], N. Kimura[171], O. Kind[16], B.T. King[73], M. King[66], R.S.B. King[118], J. Kirk[129], A.E. Kiryunin[99], T. Kishimoto[66], D. Kisielewska[38], T. Kitamura[66], T. Kittelmann[123], K. Kiuchi[160], E. Kladiva[144b], M. Klein[73], U. Klein[73], K. Kleinknecht[81], M. Klemetti[85], A. Klier[172], P. Klimek[146a,146b], A. Klimentov[25], R. Klingenberg[43], J.A. Klinger[82], E.B. Klinkby[36], T. Klioutchnikova[30], P.F. Klok[104], S. Klous[105], E.-E. Kluge[58a], T. Kluge[73], P. Kluit[105], S. Kluth[99], E. Kneringer[61], E.B.F.G. Knoops[83], A. Knue[54], B.R. Ko[45], T. Kobayashi[155], M. Kobel[44], M. Kocian[143], P. Kodys[127], K. Köneke[30], A.C. König[104], S. Koenig[81], L. Köpke[81], F. Koetsveld[104], P. Koevesarki[21], T. Koffas[29], E. Koffeman[105], L.A. Kogan[118], S. Kohlmann[175], F. Kohn[54], Z. Kohout[126], T. Kohriki[65], T. Koi[143], G.M. Kolachev[107,*], H. Kolanoski[16], V. Kolesnikov[64], I. Koletsou[89a], J. Koll[88], A.A. Komar[94], Y. Komori[155], T. Kondo[65], T. Kono[42,s], A.I. Kononov[48], R. Konoplich[108,t], N. Konstantinidis[77], R. Kopeliansky[152], S. Koperny[38], K. Korcyl[39], K. Kordas[154], A. Korn[118], A. Korol[107], I. Korolkov[12], E.V. Korolkova[139], V.A. Korotkov[128], O. Kortner[99], S. Kortner[99], V.V. Kostyukhin[21], S. Kotov[99], V.M. Kotov[64], A. Kotwal[45], C. Kourkoumelis[9], V. Kouskoura[154],

JHEP02(2013)095

A. Koutsman[159a], R. Kowalewski[169], T.Z. Kowalski[38], W. Kozanecki[136], A.S. Kozhin[128], V. Kral[126], V.A. Kramarenko[97], G. Kramberger[74], M.W. Krasny[78], A. Krasznahorkay[108], J.K. Kraus[21], A. Kravchenko[25], S. Kreiss[108], F. Krejci[126], J. Kretzschmar[73], K. Kreutzfeldt[52], N. Krieger[54], P. Krieger[158], K. Kroeninger[54], H. Kroha[99], J. Kroll[120], J. Kroseberg[21], J. Krstic[13a], U. Kruchonak[64], H. Krüger[21], T. Kruker[17], N. Krumnack[63], Z.V. Krumshteyn[64], M.K. Kruse[45], T. Kubota[86], S. Kuday[4a], S. Kuehn[48], A. Kugel[58c], T. Kuhl[42], V. Kukhtin[64], Y. Kulchitsky[90], S. Kuleshov[32b], M. Kuna[78], J. Kunkle[120], A. Kupco[125], H. Kurashige[66], M. Kurata[160], Y.A. Kurochkin[90], V. Kus[125], E.S. Kuwertz[147], M. Kuze[157], J. Kvita[142], R. Kwee[16], A. La Rosa[49], L. La Rotonda[37a,37b], L. Labarga[80], S. Lablak[135a], C. Lacasta[167], F. Lacava[132a,132b], J. Lacey[29], H. Lacker[16], D. Lacour[78], V.R. Lacuesta[167], E. Ladygin[64], R. Lafaye[5], B. Laforge[78], T. Lagouri[176], S. Lai[48], E. Laisne[55], L. Lambourne[77], C.L. Lampen[7], W. Lampl[7], E. Lancon[136], U. Landgraf[48], M.P.J. Landon[75], V.S. Lang[58a], C. Lange[42], A.J. Lankford[163], F. Lanni[25], K. Lantzsch[30], A. Lanza[119a], S. Laplace[78], C. Lapoire[21], J.F. Laporte[136], T. Lari[89a], A. Larner[118], M. Lassnig[30], P. Laurelli[47], V. Lavorini[37a,37b], W. Lavrijsen[15], P. Laycock[73], O. Le Dortz[78], E. Le Guirriec[83], E. Le Menedeu[12], T. LeCompte[6], F. Ledroit-Guillon[55], H. Lee[105], J.S.H. Lee[116], S.C. Lee[151], L. Lee[176], M. Lefebvre[169], M. Legendre[136], F. Legger[98], C. Leggett[15], M. Lehmacher[21], G. Lehmann Miotto[30], A.G. Leister[176], M.A.L. Leite[24d], R. Leitner[127], D. Lellouch[172], B. Lemmer[54], V. Lendermann[58a], K.J.C. Leney[145b], T. Lenz[105], G. Lenzen[175], B. Lenzi[30], K. Leonhardt[44], S. Leontsinis[10], F. Lepold[58a], C. Leroy[93], J-R. Lessard[169], C.G. Lester[28], C.M. Lester[120], J. Levêque[5], D. Levin[87], L.J. Levinson[172], A. Lewis[118], G.H. Lewis[108], A.M. Leyko[21], M. Leyton[16], B. Li[33b], B. Li[83], H. Li[148], H.L. Li[31], S. Li[33b,u], X. Li[87], Z. Liang[118,v], H. Liao[34], B. Liberti[133a], P. Lichard[30], K. Lie[165], W. Liebig[14], C. Limbach[21], A. Limosani[86], M. Limper[62], S.C. Lin[151,w], F. Linde[105], J.T. Linnemann[88], E. Lipeles[120], A. Lipniacka[14], T.M. Liss[165], D. Lissauer[25], A. Lister[49], A.M. Litke[137], D. Liu[151], J.B. Liu[33b], L. Liu[87], M. Liu[33b], Y. Liu[33b], M. Livan[119a,119b], S.S.A. Livermore[118], A. Lleres[55], J. Llorente Merino[80], S.L. Lloyd[75], E. Lobodzinska[42], P. Loch[7], W.S. Lockman[137], T. Loddenkoetter[21], F.K. Loebinger[82], A. Loginov[176], C.W. Loh[168], T. Lohse[16], K. Lohwasser[48], M. Lokajicek[125], V.P. Lombardo[5], R.E. Long[71], L. Lopes[124a], D. Lopez Mateos[57], J. Lorenz[98], N. Lorenzo Martinez[115], M. Losada[162], P. Loscutoff[15], F. Lo Sterzo[132a,132b], M.J. Losty[159a,*], X. Lou[41], A. Lounis[115], K.F. Loureiro[162], J. Love[6], P.A. Love[71], A.J. Lowe[143,g], F. Lu[33a], H.J. Lubatti[138], C. Luci[132a,132b], A. Lucotte[55], D. Ludwig[42], I. Ludwig[48], J. Ludwig[48], F. Luehring[60], G. Luijckx[105], W. Lukas[61], L. Luminari[132a], E. Lund[117], B. Lund-Jensen[147], B. Lundberg[79], J. Lundberg[146a,146b], O. Lundberg[146a,146b], J. Lundquist[36], M. Lungwitz[81], D. Lynn[25], E. Lytken[79], H. Ma[25], L.L. Ma[173], G. Maccarrone[47], A. Macchiolo[99], B. Maček[74], J. Machado Miguens[124a], D. Macina[30], R. Mackeprang[36], R.J. Madaras[15], H.J. Maddocks[71], W.F. Mader[44], T. Maeno[25], P. Mättig[175], S. Mättig[42], L. Magnoni[163], E. Magradze[54], K. Mahboubi[48], J. Mahlstedt[105], S. Mahmoud[73], G. Mahout[18], C. Maiani[136], C. Maidantchik[24a], A. Maio[124a,c], S. Majewski[25], Y. Makida[65], N. Makovec[115], P. Mal[136], B. Malaescu[78], Pa. Malecki[39], P. Malecki[39], V.P. Maleev[121], F. Malek[55], U. Mallik[62], D. Malon[6], C. Malone[143], S. Maltezos[10], V. Malyshev[107], S. Malyukov[30], J. Mamuzic[13b], A. Manabe[65], L. Mandelli[89a], I. Mandić[74], R. Mandrysch[62], J. Maneira[124a], A. Manfredini[99], L. Manhaes de Andrade Filho[24b], J.A. Manjarres Ramos[136], A. Mann[98], P.M. Manning[137], A. Manousakis-Katsikakis[9], B. Mansoulie[136], R. Mantifel[85], A. Mapelli[30], L. Mapelli[30], L. March[167], J.F. Marchand[29], F. Marchese[133a,133b], G. Marchiori[78], M. Marcisovsky[125], C.P. Marino[169], F. Marroquim[24a], Z. Marshall[30], L.F. Marti[17], S. Marti-Garcia[167], B. Martin[30], B. Martin[88], J.P. Martin[93], T.A. Martin[18], V.J. Martin[46], B. Martin dit Latour[49], S. Martin-Haugh[149], H. Martinez[136], M. Martinez[12], V. Martinez Outschoorn[57], A.C. Martyniuk[169], M. Marx[82], F. Marzano[132a], A. Marzin[111], L. Masetti[81], T. Mashimo[155], R. Mashinistov[94],

JHEP02(2013)095

J. Masik[82], A.L. Maslennikov[107], I. Massa[20a,20b], G. Massaro[105], N. Massol[5], P. Mastrandrea[148], A. Mastroberardino[37a,37b], T. Masubuchi[155], H. Matsunaga[155], T. Matsushita[66], C. Mattravers[118,d], J. Maurer[83], S.J. Maxfield[73], D.A. Maximov[107,h], R. Mazini[151], M. Mazur[21], L. Mazzaferro[133a,133b], M. Mazzanti[89a], J. Mc Donald[85], S.P. Mc Kee[87], A. McCarn[165], R.L. McCarthy[148], T.G. McCarthy[29], N.A. McCubbin[129], K.W. McFarlane[56,*], J.A. Mcfayden[139], G. Mchedlidze[51b], T. Mclaughlan[18], S.J. McMahon[129], R.A. McPherson[169,l], A. Meade[84], J. Mechnich[105], M. Mechtel[175], M. Medinnis[42], S. Meehan[31], R. Meera-Lebbai[111], T. Meguro[116], S. Mehlhase[36], A. Mehta[73], K. Meier[58a], B. Meirose[79], C. Melachrinos[31], B.R. Mellado Garcia[173], F. Meloni[89a,89b], L. Mendoza Navas[162], Z. Meng[151,x], A. Mengarelli[20a,20b], S. Menke[99], E. Meoni[161], K.M. Mercurio[57], P. Mermod[49], L. Merola[102a,102b], C. Meroni[89a], F.S. Merritt[31], H. Merritt[109], A. Messina[30,y], J. Metcalfe[25], A.S. Mete[163], C. Meyer[81], C. Meyer[31], J-P. Meyer[136], J. Meyer[174], J. Meyer[54], S. Michal[30], L. Micu[26a], R.P. Middleton[129], S. Migas[73], L. Mijović[136], G. Mikenberg[172], M. Mikestikova[125], M. Mikuž[74], D.W. Miller[31], R.J. Miller[88], W.J. Mills[168], C. Mills[57], A. Milov[172], D.A. Milstead[146a,146b], D. Milstein[172], A.A. Minaenko[128], M. Miñano Moya[167], I.A. Minashvili[64], A.I. Mincer[108], B. Mindur[38], M. Mineev[64], Y. Ming[173], L.M. Mir[12], G. Mirabelli[132a], J. Mitrevski[137], V.A. Mitsou[167], S. Mitsui[65], P.S. Miyagawa[139], J.U. Mjörnmark[79], T. Moa[146a,146b], V. Moeller[28], K. Mönig[42], N. Möser[21], S. Mohapatra[148], W. Mohr[48], R. Moles-Valls[167], A. Molfetas[30], J. Monk[77], E. Monnier[83], J. Montejo Berlingen[12], F. Monticelli[70], S. Monzani[20a,20b], R.W. Moore[3], G.F. Moorhead[86], C. Mora Herrera[49], A. Moraes[53], N. Morange[136], J. Morel[54], G. Morello[37a,37b], D. Moreno[81], M. Moreno Llácer[167], P. Morettini[50a], M. Morgenstern[44], M. Morii[57], A.K. Morley[30], G. Mornacchi[30], J.D. Morris[75], L. Morvaj[101], H.G. Moser[99], M. Mosidze[51b], J. Moss[109], R. Mount[143], E. Mountricha[10,z], S.V. Mouraviev[94,*], E.J.W. Moyse[84], F. Mueller[58a], J. Mueller[123], K. Mueller[21], T.A. Müller[98], T. Mueller[81], D. Muenstermann[30], Y. Munwes[153], W.J. Murray[129], I. Mussche[105], E. Musto[152], A.G. Myagkov[128], M. Myska[125], O. Nackenhorst[54], J. Nadal[12], K. Nagai[160], R. Nagai[157], K. Nagano[65], A. Nagarkar[109], Y. Nagasaka[59], M. Nagel[99], A.M. Nairz[30], Y. Nakahama[30], K. Nakamura[65], T. Nakamura[155], I. Nakano[110], G. Nanava[21], A. Napier[161], R. Narayan[58b], M. Nash[77,d], T. Nattermann[21], T. Naumann[42], G. Navarro[162], H.A. Neal[87], P.Yu. Nechaeva[94], T.J. Neep[82], A. Negri[119a,119b], G. Negri[30], M. Negrini[20a], S. Nektarijevic[49], A. Nelson[163], T.K. Nelson[143], S. Nemecek[125], P. Nemethy[108], A.A. Nepomuceno[24a], M. Nessi[30,aa], M.S. Neubauer[165], M. Neumann[175], A. Neusiedl[81], R.M. Neves[108], P. Nevski[25], F.M. Newcomer[120], P.R. Newman[18], V. Nguyen Thi Hong[136], R.B. Nickerson[118], R. Nicolaidou[136], B. Nicquevert[30], F. Niedercorn[115], J. Nielsen[137], N. Nikiforou[35], A. Nikiforov[16], V. Nikolaenko[128], I. Nikolic-Audit[78], K. Nikolics[49], K. Nikolopoulos[18], H. Nilsen[48], P. Nilsson[8], Y. Ninomiya[155], A. Nisati[132a], R. Nisius[99], T. Nobe[157], L. Nodulman[6], M. Nomachi[116], I. Nomidis[154], S. Norberg[111], M. Nordberg[30], J. Novakova[127], M. Nozaki[65], L. Nozka[113], A.-E. Nuncio-Quiroz[21], G. Nunes Hanninger[86], T. Nunnemann[98], E. Nurse[77], B.J. O'Brien[46], D.C. O'Neil[142], V. O'Shea[53], L.B. Oakes[98], F.G. Oakham[29,f], H. Oberlack[99], J. Ocariz[78], A. Ochi[66], S. Oda[69], S. Odaka[65], J. Odier[83], H. Ogren[60], A. Oh[82], S.H. Oh[45], C.C. Ohm[30], T. Ohshima[101], W. Okamura[116], H. Okawa[25], Y. Okumura[31], T. Okuyama[155], A. Olariu[26a], A.G. Olchevski[64], S.A. Olivares Pino[32a], M. Oliveira[124a,i], D. Oliveira Damazio[25], E. Oliver Garcia[167], D. Olivito[120], A. Olszewski[39], J. Olszowska[39], A. Onofre[124a,ab], P.U.E. Onyisi[31,ac], C.J. Oram[159a], M.J. Oreglia[31], Y. Oren[153], D. Orestano[134a,134b], N. Orlando[72a,72b], C. Oropeza Barrera[53], R.S. Orr[158], B. Osculati[50a,50b], R. Ospanov[120], C. Osuna[12], G. Otero y Garzon[27], J.P. Ottersbach[105], M. Ouchrif[135d], E.A. Ouellette[169], F. Ould-Saada[117], A. Ouraou[136], Q. Ouyang[33a], A. Ovcharova[15], M. Owen[82], S. Owen[139], V.E. Ozcan[19a], N. Ozturk[8], A. Pacheco Pages[12], C. Padilla Aranda[12], S. Pagan Griso[15], E. Paganis[139], C. Pahl[99], F. Paige[25], P. Pais[84], K. Pajchel[117], G. Palacino[159b],

JHEP02(2013)095

C.P. Paleari[7], S. Palestini[30], D. Pallin[34], A. Palma[124a], J.D. Palmer[18], Y.B. Pan[173], E. Panagiotopoulou[10], J.G. Panduro Vazquez[76], P. Pani[105], N. Panikashvili[87], S. Panitkin[25], D. Pantea[26a], A. Papadelis[146a], Th.D. Papadopoulou[10], A. Paramonov[6], D. Paredes Hernandez[34], W. Park[25,ad], M.A. Parker[28], F. Parodi[50a,50b], J.A. Parsons[35], U. Parzefall[48], S. Pashapour[54], E. Pasqualucci[132a], S. Passaggio[50a], A. Passeri[134a], F. Pastore[134a,134b,*], Fr. Pastore[76], G. Pásztor[49,ae], S. Pataraia[175], N. Patel[150], J.R. Pater[82], S. Patricelli[102a,102b], T. Pauly[30], S. Pedraza Lopez[167], M.I. Pedraza Morales[173], S.V. Peleganchuk[107], D. Pelikan[166], H. Peng[33b], B. Penning[31], A. Penson[35], J. Penwell[60], M. Perantoni[24a], K. Perez[35,af], T. Perez Cavalcanti[42], E. Perez Codina[159a], M.T. Pérez García-Estañ[167], V. Perez Reale[35], L. Perini[89a,89b], H. Pernegger[30], R. Perrino[72a], P. Perrodo[5], V.D. Peshekhonov[64], K. Peters[30], B.A. Petersen[30], J. Petersen[30], T.C. Petersen[36], E. Petit[5], A. Petridis[154], C. Petridou[154], E. Petrolo[132a], F. Petrucci[134a,134b], D. Petschull[42], M. Petteni[142], R. Pezoa[32b], A. Phan[86], P.W. Phillips[129], G. Piacquadio[30], A. Picazio[49], E. Piccaro[75], M. Piccinini[20a,20b], S.M. Piec[42], R. Piegaia[27], D.T. Pignotti[109], J.E. Pilcher[31], A.D. Pilkington[82], J. Pina[124a,c], M. Pinamonti[164a,164c], A. Pinder[118], J.L. Pinfold[3], A. Pingel[36], B. Pinto[124a], C. Pizio[89a,89b], M.-A. Pleier[25], E. Plotnikova[64], A. Poblaguev[25], S. Poddar[58a], F. Podlyski[34], L. Poggioli[115], D. Pohl[21], M. Pohl[49], G. Polesello[119a], A. Policicchio[37a,37b], R. Polifka[158], A. Polini[20a], J. Poll[75], V. Polychronakos[25], D. Pomeroy[23], K. Pommès[30], L. Pontecorvo[132a], B.G. Pope[88], G.A. Popeneciu[26a], D.S. Popovic[13a], A. Poppleton[30], X. Portell Bueso[30], G.E. Pospelov[99], S. Pospisil[126], I.N. Potrap[99], C.J. Potter[149], C.T. Potter[114], G. Poulard[30], J. Poveda[60], V. Pozdnyakov[64], R. Prabhu[77], P. Pralavorio[83], A. Pranko[15], S. Prasad[30], R. Pravahan[25], S. Prell[63], K. Pretzl[17], D. Price[60], J. Price[73], L.E. Price[6], D. Prieur[123], M. Primavera[72a], K. Prokofiev[108], F. Prokoshin[32b], S. Protopopescu[25], J. Proudfoot[6], X. Prudent[44], M. Przybycien[38], H. Przysiezniak[5], S. Psoroulas[21], E. Ptacek[114], E. Pueschel[84], D. Puldon[148], J. Purdham[87], M. Purohit[25,ad], P. Puzo[115], Y. Pylypchenko[62], J. Qian[87], A. Quadt[54], D.R. Quarrie[15], W.B. Quayle[173], M. Raas[104], V. Radeka[25], V. Radescu[42], P. Radloff[114], F. Ragusa[89a,89b], G. Rahal[178], A.M. Rahimi[109], D. Rahm[25], S. Rajagopalan[25], M. Rammensee[48], M. Rammes[141], A.S. Randle-Conde[40], K. Randrianarivony[29], K. Rao[163], F. Rauscher[98], T.C. Rave[48], M. Raymond[30], A.L. Read[117], D.M. Rebuzzi[119a,119b], A. Redelbach[174], G. Redlinger[25], R. Reece[120], K. Reeves[41], A. Reinsch[114], I. Reisinger[43], C. Rembser[30], Z.L. Ren[151], A. Renaud[115], M. Rescigno[132a], S. Resconi[89a], B. Resende[136], P. Reznicek[98], R. Rezvani[158], R. Richter[99], E. Richter-Was[5,ag], M. Ridel[78], M. Rijssenbeek[148], A. Rimoldi[119a,119b], L. Rinaldi[20a], R.R. Rios[40], E. Ritsch[61], I. Riu[12], G. Rivoltella[89a,89b], F. Rizatdinova[112], E. Rizvi[75], S.H. Robertson[85,l], A. Robichaud-Veronneau[118], D. Robinson[28], J.E.M. Robinson[82], A. Robson[53], J.G. Rocha de Lima[106], C. Roda[122a,122b], D. Roda Dos Santos[30], A. Roe[54], S. Roe[30], O. Røhne[117], S. Rolli[161], A. Romaniouk[96], M. Romano[20a,20b], G. Romeo[27], E. Romero Adam[167], N. Rompotis[138], L. Roos[78], E. Ros[167], S. Rosati[132a], K. Rosbach[49], A. Rose[149], M. Rose[76], G.A. Rosenbaum[158], P.L. Rosendahl[14], O. Rosenthal[141], L. Rosselet[49], V. Rossetti[12], E. Rossi[132a,132b], L.P. Rossi[50a], M. Rotaru[26a], I. Roth[172], J. Rothberg[138], D. Rousseau[115], C.R. Royon[136], A. Rozanov[83], Y. Rozen[152], X. Ruan[33a,ah], F. Rubbo[12], I. Rubinskiy[42], N. Ruckstuhl[105], V.I. Rud[97], C. Rudolph[44], F. Rühr[7], A. Ruiz-Martinez[63], L. Rumyantsev[64], Z. Rurikova[48], N.A. Rusakovich[64], A. Ruschke[98], J.P. Rutherfoord[7], N. Ruthmann[48], P. Ruzicka[125], Y.F. Ryabov[121], M. Rybar[127], G. Rybkin[115], N.C. Ryder[118], A.F. Saavedra[150], I. Sadeh[153], H.F-W. Sadrozinski[137], R. Sadykov[64], F. Safai Tehrani[132a], H. Sakamoto[155], G. Salamanna[75], A. Salamon[133a], M. Saleem[111], D. Salek[30], D. Salihagic[99], A. Salnikov[143], J. Salt[167], B.M. Salvachua Ferrando[6], D. Salvatore[37a,37b], F. Salvatore[149], A. Salvucci[104], A. Salzburger[30], D. Sampsonidis[154], B.H. Samset[117], A. Sanchez[102a,102b], V. Sanchez Martinez[167], H. Sandaker[14], H.G. Sander[81], M.P. Sanders[98], M. Sandhoff[175],

JHEP02(2013)095

T. Sandoval[28], C. Sandoval[162], R. Sandstroem[99], D.P.C. Sankey[129], A. Sansoni[47], C. Santamarina Rios[85], C. Santoni[34], R. Santonico[133a,133b], H. Santos[124a], I. Santoyo Castillo[149], J.G. Saraiva[124a], T. Sarangi[173], E. Sarkisyan-Grinbaum[8], B. Sarrazin[21], F. Sarri[122a,122b], G. Sartisohn[175], O. Sasaki[65], Y. Sasaki[155], N. Sasao[67], I. Satsounkevitch[90], G. Sauvage[5,*], E. Sauvan[5], J.B. Sauvan[115], P. Savard[158,f], V. Savinov[123], D.O. Savu[30], L. Sawyer[25,n], D.H. Saxon[53], J. Saxon[120], C. Sbarra[20a], A. Sbrizzi[20a,20b], D.A. Scannicchio[163], M. Scarcella[150], J. Schaarschmidt[115], P. Schacht[99], D. Schaefer[120], U. Schäfer[81], A. Schaelicke[46], S. Schaepe[21], S. Schaetzel[58b], A.C. Schaffer[115], D. Schaile[98], R.D. Schamberger[148], V. Scharf[58a], V.A. Schegelsky[121], D. Scheirich[87], M. Schernau[163], M.I. Scherzer[35], C. Schiavi[50a,50b], J. Schieck[98], M. Schioppa[37a,37b], S. Schlenker[30], E. Schmidt[48], K. Schmieden[21], C. Schmitt[81], S. Schmitt[58b], B. Schneider[17], U. Schnoor[44], L. Schoeffel[136], A. Schoening[58b], A.L.S. Schorlemmer[54], M. Schott[30], D. Schouten[159a], J. Schovancova[125], M. Schram[85], C. Schroeder[81], N. Schroer[58c], M.J. Schultens[21], J. Schultes[175], H.-C. Schultz-Coulon[58a], H. Schulz[16], M. Schumacher[48], B.A. Schumm[137], Ph. Schune[136], A. Schwartzman[143], Ph. Schwegler[99], Ph. Schwemling[78], R. Schwienhorst[88], J. Schwindling[136], T. Schwindt[21], M. Schwoerer[5], F.G. Sciacca[17], E. Scifo[115], G. Sciolla[23], W.G. Scott[129], J. Searcy[114], G. Sedov[42], E. Sedykh[121], S.C. Seidel[103], A. Seiden[137], F. Seifert[44], J.M. Seixas[24a], G. Sekhniaidze[102a], S.J. Sekula[40], K.E. Selbach[46], D.M. Seliverstov[121], B. Sellden[146a], G. Sellers[73], M. Seman[144b], N. Semprini-Cesari[20a,20b], C. Serfon[30], L. Serin[115], L. Serkin[54], R. Seuster[159a], H. Severini[111], A. Sfyrla[30], E. Shabalina[54], M. Shamim[114], L.Y. Shan[33a], J.T. Shank[22], Q.T. Shao[86], M. Shapiro[15], P.B. Shatalov[95], K. Shaw[164a,164c], D. Sherman[176], P. Sherwood[77], S. Shimizu[101], M. Shimojima[100], T. Shin[56], M. Shiyakova[64], A. Shmeleva[94], M.J. Shochet[31], D. Short[118], S. Shrestha[63], E. Shulga[96], M.A. Shupe[7], P. Sicho[125], A. Sidoti[132a], F. Siegert[48], Dj. Sijacki[13a], O. Silbert[172], J. Silva[124a], Y. Silver[153], D. Silverstein[143], S.B. Silverstein[146a], V. Simak[126], O. Simard[136], Lj. Simic[13a], S. Simion[115], E. Simioni[81], B. Simmons[77], R. Simoniello[89a,89b], M. Simonyan[36], P. Sinervo[158], N.B. Sinev[114], V. Sipica[141], G. Siragusa[174], A. Sircar[25], A.N. Sisakyan[64,*], S.Yu. Sivoklokov[97], J. Sjölin[146a,146b], T.B. Sjursen[14], L.A. Skinnari[15], H.P. Skottowe[57], K. Skovpen[107], P. Skubic[111], M. Slater[18], T. Slavicek[126], K. Sliwa[161], V. Smakhtin[172], B.H. Smart[46], L. Smestad[117], S.Yu. Smirnov[96], Y. Smirnov[96], L.N. Smirnova[97,ai], O. Smirnova[79], B.C. Smith[57], K.M. Smith[53], M. Smizanska[71], K. Smolek[126], A.A. Snesarev[94], S.W. Snow[82], J. Snow[111], S. Snyder[25], R. Sobie[169,l], J. Sodomka[126], A. Soffer[153], C.A. Solans[30], M. Solar[126], J. Solc[126], E.Yu. Soldatov[96], U. Soldevila[167], E. Solfaroli Camillocci[132a,132b], A.A. Solodkov[128], O.V. Solovyanov[128], V. Solovyev[121], N. Soni[1], A. Sood[15], V. Sopko[126], B. Sopko[126], M. Sosebee[8], R. Soualah[164a,164c], P. Soueid[93], A. Soukharev[107], D. South[42], S. Spagnolo[72a,72b], F. Spanò[76], R. Spighi[20a], G. Spigo[30], R. Spiwoks[30], M. Spousta[127,aj], T. Spreitzer[158], B. Spurlock[8], R.D. St. Denis[53], J. Stahlman[120], R. Stamen[58a], E. Stanecka[39], R.W. Stanek[6], C. Stanescu[134a], M. Stanescu-Bellu[42], M.M. Stanitzki[42], S. Stapnes[117], E.A. Starchenko[128], J. Stark[55], P. Staroba[125], P. Starovoitov[42], R. Staszewski[39], A. Staude[98], P. Stavina[144a,*], G. Steele[53], P. Steinbach[44], P. Steinberg[25], I. Stekl[126], B. Stelzer[142], H.J. Stelzer[88], O. Stelzer-Chilton[159a], H. Stenzel[52], S. Stern[99], G.A. Stewart[30], J.A. Stillings[21], M.C. Stockton[85], M. Stoebe[85], K. Stoerig[48], G. Stoicea[26a], S. Stonjek[99], P. Strachota[127], A.R. Stradling[8], A. Straessner[44], J. Strandberg[147], S. Strandberg[146a,146b], A. Strandlie[117], M. Strang[109], E. Strauss[143], M. Strauss[111], P. Strizenec[144b], R. Ströhmer[174], D.M. Strom[114], J.A. Strong[76,*], R. Stroynowski[40], B. Stugu[14], I. Stumer[25,*], J. Stupak[148], P. Sturm[175], N.A. Styles[42], D.A. Soh[151,v], D. Su[143], HS. Subramania[3], R. Subramaniam[25], A. Succurro[12], Y. Sugaya[116], C. Suhr[106], M. Suk[127], V.V. Sulin[94], S. Sultansoy[4d], T. Sumida[67], X. Sun[55], J.E. Sundermann[48], K. Suruliz[139], G. Susinno[37a,37b], M.R. Sutton[149], Y. Suzuki[65], Y. Suzuki[66], M. Svatos[125], S. Swedish[168], I. Sykora[144a], T. Sykora[127],

JHEP02(2013)095

J. Sánchez[167], D. Ta[105], K. Tackmann[42], A. Taffard[163], R. Tafirout[159a], N. Taiblum[153], Y. Takahashi[101], H. Takai[25], R. Takashima[68], H. Takeda[66], T. Takeshita[140], Y. Takubo[65], M. Talby[83], A. Talyshev[107,h], M.C. Tamsett[25], K.G. Tan[86], J. Tanaka[155], R. Tanaka[115], S. Tanaka[131], S. Tanaka[65], A.J. Tanasijczuk[142], K. Tani[66], N. Tannoury[83], S. Tapprogge[81], D. Tardif[158], S. Tarem[152], F. Tarrade[29], G.F. Tartarelli[89a], P. Tas[127], M. Tasevsky[125], E. Tassi[37a,37b], Y. Tayalati[135d], C. Taylor[77], F.E. Taylor[92], G.N. Taylor[86], W. Taylor[159b], M. Teinturier[115], F.A. Teischinger[30], M. Teixeira Dias Castanheira[75], P. Teixeira-Dias[76], K.K. Temming[48], H. Ten Kate[30], P.K. Teng[151], S. Terada[65], K. Terashi[155], J. Terron[80], M. Testa[47], R.J. Teuscher[158,l], J. Therhaag[21], T. Theveneaux-Pelzer[78], S. Thoma[48], J.P. Thomas[18], E.N. Thompson[35], P.D. Thompson[18], P.D. Thompson[158], A.S. Thompson[53], L.A. Thomsen[36], E. Thomson[120], M. Thomson[28], W.M. Thong[86], R.P. Thun[87], F. Tian[35], M.J. Tibbetts[15], T. Tic[125], V.O. Tikhomirov[94], Y.A. Tikhonov[107,h], S. Timoshenko[96], E. Tiouchichine[83], P. Tipton[176], S. Tisserant[83], T. Todorov[5], S. Todorova-Nova[161], B. Toggerson[163], J. Tojo[69], S. Tokár[144a], K. Tokushuku[65], K. Tollefson[88], M. Tomoto[101], L. Tompkins[31], K. Toms[103], A. Tonoyan[14], C. Topfel[17], N.D. Topilin[64], E. Torrence[114], H. Torres[78], E. Torró Pastor[167], J. Toth[83,ae], F. Touchard[83], D.R. Tovey[139], T. Trefzger[174], L. Tremblet[30], A. Tricoli[30], I.M. Trigger[159a], S. Trincaz-Duvoid[78], M.F. Tripiana[70], N. Triplett[25], W. Trischuk[158], B. Trocmé[55], C. Troncon[89a], M. Trottier-McDonald[142], P. True[88], M. Trzebinski[39], A. Trzupek[39], C. Tsarouchas[30], J.C-L. Tseng[118], M. Tsiakiris[105], P.V. Tsiareshka[90], D. Tsionou[5,ak], G. Tsipolitis[10], S. Tsiskaridze[12], V. Tsiskaridze[48], E.G. Tskhadadze[51a], I.I. Tsukerman[95], V. Tsulaia[15], J.-W. Tsung[21], S. Tsuno[65], D. Tsybychev[148], A. Tua[139], A. Tudorache[26a], V. Tudorache[26a], J.M. Tuggle[31], M. Turala[39], D. Turecek[126], I. Turk Cakir[4e], R. Turra[89a,89b], P.M. Tuts[35], A. Tykhonov[74], M. Tylmad[146a,146b], M. Tyndel[129], G. Tzanakos[9], K. Uchida[21], I. Ueda[155], R. Ueno[29], M. Ughetto[83], M. Ugland[14], M. Uhlenbrock[21], F. Ukegawa[160], G. Unal[30], A. Undrus[25], G. Unel[163], Y. Unno[65], D. Urbaniec[35], P. Urquijo[21], G. Usai[8], L. Vacavant[83], V. Vacek[126], B. Vachon[85], S. Vahsen[15], S. Valentinetti[20a,20b], A. Valero[167], L. Valery[34], S. Valkar[127], E. Valladolid Gallego[167], S. Vallecorsa[152], J.A. Valls Ferrer[167], R. Van Berg[120], P.C. Van Der Deijl[105], R. van der Geer[105], H. van der Graaf[105], R. Van Der Leeuw[105], E. van der Poel[105], D. van der Ster[30], N. van Eldik[30], P. van Gemmeren[6], J. Van Nieuwkoop[142], I. van Vulpen[105], M. Vanadia[99], W. Vandelli[30], A. Vaniachine[6], P. Vankov[42], F. Vannucci[78], R. Vari[132a], E.W. Varnes[7], T. Varol[84], D. Varouchas[15], A. Vartapetian[8], K.E. Varvell[150], V.I. Vassilakopoulos[56], F. Vazeille[34], T. Vazquez Schroeder[54], G. Vegni[89a,89b], J.J. Veillet[115], F. Veloso[124a], R. Veness[30], S. Veneziano[132a], A. Ventura[72a,72b], D. Ventura[84], M. Venturi[48], N. Venturi[158], V. Vercesi[119a], M. Verducci[138], W. Verkerke[105], J.C. Vermeulen[105], A. Vest[44], M.C. Vetterli[142,f], I. Vichou[165], T. Vickey[145b,al], O.E. Vickey Boeriu[145b], G.H.A. Viehhauser[118], S. Viel[168], M. Villa[20a,20b], M. Villaplana Perez[167], E. Vilucchi[47], M.G. Vincter[29], E. Vinek[30], V.B. Vinogradov[64], M. Virchaux[136,*], J. Virzi[15], O. Vitells[172], M. Viti[42], I. Vivarelli[48], F. Vives Vaque[3], S. Vlachos[10], D. Vladoiu[98], M. Vlasak[126], A. Vogel[21], P. Vokac[126], G. Volpi[47], M. Volpi[86], G. Volpini[89a], H. von der Schmitt[99], H. von Radziewski[48], E. von Toerne[21], V. Vorobel[127], V. Vorwerk[12], M. Vos[167], R. Voss[30], J.H. Vossebeld[73], N. Vranjes[136], M. Vranjes Milosavljevic[105], V. Vrba[125], M. Vreeswijk[105], T. Vu Anh[48], R. Vuillermet[30], I. Vukotic[31], W. Wagner[175], P. Wagner[21], H. Wahlen[175], S. Wahrmund[44], J. Wakabayashi[101], S. Walch[87], J. Walder[71], R. Walker[98], W. Walkowiak[141], R. Wall[176], P. Waller[73], B. Walsh[176], C. Wang[45], H. Wang[173], H. Wang[40], J. Wang[151], J. Wang[33a], R. Wang[103], S.M. Wang[151], T. Wang[21], A. Warburton[85], C.P. Ward[28], D.R. Wardrope[77], M. Warsinsky[48], A. Washbrook[46], C. Wasicki[42], I. Watanabe[66], P.M. Watkins[18], A.T. Watson[18], I.J. Watson[150], M.F. Watson[18], G. Watts[138], S. Watts[82], A.T. Waugh[150], B.M. Waugh[77], M.S. Weber[17], J.S. Webster[31], A.R. Weidberg[118], P. Weigell[99],

JHEP02(2013)095

J. Weingarten[54], C. Weiser[48], P.S. Wells[30], T. Wenaus[25], D. Wendland[16], Z. Weng[151,v], T. Wengler[30], S. Wenig[30], N. Wermes[21], M. Werner[48], P. Werner[30], M. Werth[163], M. Wessels[58a], J. Wetter[161], C. Weydert[55], K. Whalen[29], A. White[8], M.J. White[86], S. White[122a,122b], S.R. Whitehead[118], D. Whiteson[163], D. Whittington[60], D. Wicke[175], F.J. Wickens[129], W. Wiedenmann[173], M. Wielers[129], P. Wienemann[21], C. Wiglesworth[75], L.A.M. Wiik-Fuchs[21], P.A. Wijeratne[77], A. Wildauer[99], M.A. Wildt[42,s], I. Wilhelm[127], H.G. Wilkens[30], J.Z. Will[98], E. Williams[35], H.H. Williams[120], S. Williams[28], W. Willis[35], S. Willocq[84], J.A. Wilson[18], M.G. Wilson[143], A. Wilson[87], I. Wingerter-Seez[5], S. Winkelmann[48], F. Winklmeier[30], M. Wittgen[143], S.J. Wollstadt[81], M.W. Wolter[39], H. Wolters[124a,i], W.C. Wong[41], G. Wooden[87], B.K. Wosiek[39], J. Wotschack[30], M.J. Woudstra[82], K.W. Wozniak[39], K. Wraight[53], M. Wright[53], B. Wrona[73], S.L. Wu[173], X. Wu[49], Y. Wu[33b,am], E. Wulf[35], B.M. Wynne[46], S. Xella[36], M. Xiao[136], S. Xie[48], C. Xu[33b,z], D. Xu[33a], L. Xu[33b], B. Yabsley[150], S. Yacoob[145a,an], M. Yamada[65], H. Yamaguchi[155], A. Yamamoto[65], K. Yamamoto[63], S. Yamamoto[155], T. Yamamura[155], T. Yamanaka[155], K. Yamauchi[101], T. Yamazaki[155], Y. Yamazaki[66], Z. Yan[22], H. Yang[33e], H. Yang[173], U.K. Yang[82], Y. Yang[109], Z. Yang[146a,146b], S. Yanush[91], L. Yao[33a], Y. Yasu[65], E. Yatsenko[42], J. Ye[40], S. Ye[25], A.L. Yen[57], M. Yilmaz[4c], R. Yoosoofmiya[123], K. Yorita[171], R. Yoshida[6], K. Yoshihara[155], C. Young[143], C.J. Young[118], S. Youssef[22], D. Yu[25], D.R. Yu[15], J. Yu[8], J. Yu[112], L. Yuan[66], A. Yurkewicz[106], B. Zabinski[39], R. Zaidan[62], A.M. Zaitsev[128], L. Zanello[132a,132b], D. Zanzi[99], A. Zaytsev[25], C. Zeitnitz[175], M. Zeman[126], A. Zemla[39], O. Zenin[128], T. Ženiš[144a], Z. Zinonos[122a,122b], D. Zerwas[115], G. Zevi della Porta[57], D. Zhang[87], H. Zhang[88], J. Zhang[6], X. Zhang[33d], Z. Zhang[115], L. Zhao[108], Z. Zhao[33b], A. Zhemchugov[64], J. Zhong[118], B. Zhou[87], N. Zhou[163], Y. Zhou[151], C.G. Zhu[33d], H. Zhu[42], J. Zhu[87], Y. Zhu[33b], X. Zhuang[98], V. Zhuravlov[99], A. Zibell[98], D. Zieminska[60], N.I. Zimin[64], R. Zimmermann[21], S. Zimmermann[21], S. Zimmermann[48], M. Ziolkowski[141], R. Zitoun[5], L. Živković[35], V.V. Zmouchko[128,*], G. Zobernig[173], A. Zoccoli[20a,20b], M. zur Nedden[16], V. Zutshi[106], L. Zwalinski[30]

[1] School of Chemistry and Physics, University of Adelaide, Adelaide, Australia

[2] Physics Department, SUNY Albany, Albany NY, United States of America

[3] Department of Physics, University of Alberta, Edmonton AB, Canada

[4] [(a)] Department of Physics, Ankara University, Ankara; [(b)] Department of Physics, Dumlupinar University, Kutahya; [(c)] Department of Physics, Gazi University, Ankara; [(d)] Division of Physics, TOBB University of Economics and Technology, Ankara; [(e)] Turkish Atomic Energy Authority, Ankara, Turkey

[5] LAPP, CNRS/IN2P3 and Université de Savoie, Annecy-le-Vieux, France

[6] High Energy Physics Division, Argonne National Laboratory, Argonne IL, United States of America

[7] Department of Physics, University of Arizona, Tucson AZ, United States of America

[8] Department of Physics, The University of Texas at Arlington, Arlington TX, United States of America

[9] Physics Department, University of Athens, Athens, Greece

[10] Physics Department, National Technical University of Athens, Zografou, Greece

[11] Institute of Physics, Azerbaijan Academy of Sciences, Baku, Azerbaijan

[12] Institut de Física d'Altes Energies and Departament de Física de la Universitat Autònoma de Barcelona and ICREA, Barcelona, Spain

[13] [(a)] Institute of Physics, University of Belgrade, Belgrade; [(b)] Vinca Institute of Nuclear Sciences, University of Belgrade, Belgrade, Serbia

[14] Department for Physics and Technology, University of Bergen, Bergen, Norway

[15] Physics Division, Lawrence Berkeley National Laboratory and University of California, Berkeley CA, United States of America

[16] Department of Physics, Humboldt University, Berlin, Germany

[17] Albert Einstein Center for Fundamental Physics and Laboratory for High Energy Physics, University of Bern, Bern, Switzerland

JHEP02(2013)095

[18] School of Physics and Astronomy, University of Birmingham, Birmingham, United Kingdom
[19] [(a)] Department of Physics, Bogazici University, Istanbul; [(b)] Division of Physics, Dogus University, Istanbul; [(c)] Department of Physics Engineering, Gaziantep University, Gaziantep; [(d)] Department of Physics, Istanbul Technical University, Istanbul, Turkey
[20] [(a)] INFN Sezione di Bologna; [(b)] Dipartimento di Fisica, Università di Bologna, Bologna, Italy
[21] Physikalisches Institut, University of Bonn, Bonn, Germany
[22] Department of Physics, Boston University, Boston MA, United States of America
[23] Department of Physics, Brandeis University, Waltham MA, United States of America
[24] [(a)] Universidade Federal do Rio De Janeiro COPPE/EE/IF, Rio de Janeiro; [(b)] Federal University of Juiz de Fora (UFJF), Juiz de Fora; [(c)] Federal University of Sao Joao del Rei (UFSJ), Sao Joao del Rei; [(d)] Instituto de Fisica, Universidade de Sao Paulo, Sao Paulo, Brazil
[25] Physics Department, Brookhaven National Laboratory, Upton NY, United States of America
[26] [(a)] National Institute of Physics and Nuclear Engineering, Bucharest; [(b)] University Politehnica Bucharest, Bucharest; [(c)] West University in Timisoara, Timisoara, Romania
[27] Departamento de Física, Universidad de Buenos Aires, Buenos Aires, Argentina
[28] Cavendish Laboratory, University of Cambridge, Cambridge, United Kingdom
[29] Department of Physics, Carleton University, Ottawa ON, Canada
[30] CERN, Geneva, Switzerland
[31] Enrico Fermi Institute, University of Chicago, Chicago IL, United States of America
[32] [(a)] Departamento de Física, Pontificia Universidad Católica de Chile, Santiago; [(b)] Departamento de Física, Universidad Técnica Federico Santa María, Valparaíso, Chile
[33] [(a)] Institute of High Energy Physics, Chinese Academy of Sciences, Beijing; [(b)] Department of Modern Physics, University of Science and Technology of China, Anhui; [(c)] Department of Physics, Nanjing University, Jiangsu; [(d)] School of Physics, Shandong University, Shandong; [(e)] Physics Department, Shanghai Jiao Tong University, Shanghai, China
[34] Laboratoire de Physique Corpusculaire, Clermont Université and Université Blaise Pascal and CNRS/IN2P3, Clermont-Ferrand, France
[35] Nevis Laboratory, Columbia University, Irvington NY, United States of America
[36] Niels Bohr Institute, University of Copenhagen, Kobenhavn, Denmark
[37] [(a)] INFN Gruppo Collegato di Cosenza; [(b)] Dipartimento di Fisica, Università della Calabria, Arcavata di Rende, Italy
[38] AGH University of Science and Technology, Faculty of Physics and Applied Computer Science, Krakow, Poland
[39] The Henryk Niewodniczanski Institute of Nuclear Physics, Polish Academy of Sciences, Krakow, Poland
[40] Physics Department, Southern Methodist University, Dallas TX, United States of America
[41] Physics Department, University of Texas at Dallas, Richardson TX, United States of America
[42] DESY, Hamburg and Zeuthen, Germany
[43] Institut für Experimentelle Physik IV, Technische Universität Dortmund, Dortmund, Germany
[44] Institut für Kern- und Teilchenphysik, Technical University Dresden, Dresden, Germany
[45] Department of Physics, Duke University, Durham NC, United States of America
[46] SUPA - School of Physics and Astronomy, University of Edinburgh, Edinburgh, United Kingdom
[47] INFN Laboratori Nazionali di Frascati, Frascati, Italy
[48] Fakultät für Mathematik und Physik, Albert-Ludwigs-Universität, Freiburg, Germany
[49] Section de Physique, Université de Genève, Geneva, Switzerland
[50] [(a)] INFN Sezione di Genova; [(b)] Dipartimento di Fisica, Università di Genova, Genova, Italy
[51] [(a)] E. Andronikashvili Institute of Physics, Iv. Javakhishvili Tbilisi State University, Tbilisi; [(b)] High Energy Physics Institute, Tbilisi State University, Tbilisi, Georgia
[52] II Physikalisches Institut, Justus-Liebig-Universität Giessen, Giessen, Germany
[53] SUPA - School of Physics and Astronomy, University of Glasgow, Glasgow, United Kingdom
[54] II Physikalisches Institut, Georg-August-Universität, Göttingen, Germany
[55] Laboratoire de Physique Subatomique et de Cosmologie, Université Joseph Fourier and CNRS/IN2P3 and Institut National Polytechnique de Grenoble, Grenoble, France

JHEP02(2013)095

[56] Department of Physics, Hampton University, Hampton VA, United States of America
[57] Laboratory for Particle Physics and Cosmology, Harvard University, Cambridge MA, United States of America
[58] [(a)] Kirchhoff-Institut für Physik, Ruprecht-Karls-Universität Heidelberg, Heidelberg; [(b)] Physikalisches Institut, Ruprecht-Karls-Universität Heidelberg, Heidelberg; [(c)] ZITI Institut für technische Informatik, Ruprecht-Karls-Universität Heidelberg, Mannheim, Germany
[59] Faculty of Applied Information Science, Hiroshima Institute of Technology, Hiroshima, Japan
[60] Department of Physics, Indiana University, Bloomington IN, United States of America
[61] Institut für Astro- und Teilchenphysik, Leopold-Franzens-Universität, Innsbruck, Austria
[62] University of Iowa, Iowa City IA, United States of America
[63] Department of Physics and Astronomy, Iowa State University, Ames IA, United States of America
[64] Joint Institute for Nuclear Research, JINR Dubna, Dubna, Russia
[65] KEK, High Energy Accelerator Research Organization, Tsukuba, Japan
[66] Graduate School of Science, Kobe University, Kobe, Japan
[67] Faculty of Science, Kyoto University, Kyoto, Japan
[68] Kyoto University of Education, Kyoto, Japan
[69] Department of Physics, Kyushu University, Fukuoka, Japan
[70] Instituto de Física La Plata, Universidad Nacional de La Plata and CONICET, La Plata, Argentina
[71] Physics Department, Lancaster University, Lancaster, United Kingdom
[72] [(a)] INFN Sezione di Lecce; [(b)] Dipartimento di Matematica e Fisica, Università del Salento, Lecce, Italy
[73] Oliver Lodge Laboratory, University of Liverpool, Liverpool, United Kingdom
[74] Department of Physics, Jožef Stefan Institute and University of Ljubljana, Ljubljana, Slovenia
[75] School of Physics and Astronomy, Queen Mary University of London, London, United Kingdom
[76] Department of Physics, Royal Holloway University of London, Surrey, United Kingdom
[77] Department of Physics and Astronomy, University College London, London, United Kingdom
[78] Laboratoire de Physique Nucléaire et de Hautes Energies, UPMC and Université Paris-Diderot and CNRS/IN2P3, Paris, France
[79] Fysiska institutionen, Lunds universitet, Lund, Sweden
[80] Departamento de Fisica Teorica C-15, Universidad Autonoma de Madrid, Madrid, Spain
[81] Institut für Physik, Universität Mainz, Mainz, Germany
[82] School of Physics and Astronomy, University of Manchester, Manchester, United Kingdom
[83] CPPM, Aix-Marseille Université and CNRS/IN2P3, Marseille, France
[84] Department of Physics, University of Massachusetts, Amherst MA, United States of America
[85] Department of Physics, McGill University, Montreal QC, Canada
[86] School of Physics, University of Melbourne, Victoria, Australia
[87] Department of Physics, The University of Michigan, Ann Arbor MI, United States of America
[88] Department of Physics and Astronomy, Michigan State University, East Lansing MI, United States of America
[89] [(a)] INFN Sezione di Milano; [(b)] Dipartimento di Fisica, Università di Milano, Milano, Italy
[90] B.I. Stepanov Institute of Physics, National Academy of Sciences of Belarus, Minsk, Republic of Belarus
[91] National Scientific and Educational Centre for Particle and High Energy Physics, Minsk, Republic of Belarus
[92] Department of Physics, Massachusetts Institute of Technology, Cambridge MA, United States of America
[93] Group of Particle Physics, University of Montreal, Montreal QC, Canada
[94] P.N. Lebedev Institute of Physics, Academy of Sciences, Moscow, Russia
[95] Institute for Theoretical and Experimental Physics (ITEP), Moscow, Russia
[96] Moscow Engineering and Physics Institute (MEPhI), Moscow, Russia
[97] D.V.Skobeltsyn Institute of Nuclear Physics, M.V.Lomonosov Moscow State University, Moscow, Russia

JHEP02(2013)095

[98] Fakultät für Physik, Ludwig-Maximilians-Universität München, München, Germany
[99] Max-Planck-Institut für Physik (Werner-Heisenberg-Institut), München, Germany
[100] Nagasaki Institute of Applied Science, Nagasaki, Japan
[101] Graduate School of Science and Kobayashi-Maskawa Institute, Nagoya University, Nagoya, Japan
[102] [(a)] INFN Sezione di Napoli; [(b)] Dipartimento di Scienze Fisiche, Università di Napoli, Napoli, Italy
[103] Department of Physics and Astronomy, University of New Mexico, Albuquerque NM, United States of America
[104] Institute for Mathematics, Astrophysics and Particle Physics, Radboud University Nijmegen/Nikhef, Nijmegen, Netherlands
[105] Nikhef National Institute for Subatomic Physics and University of Amsterdam, Amsterdam, Netherlands
[106] Department of Physics, Northern Illinois University, DeKalb IL, United States of America
[107] Budker Institute of Nuclear Physics, SB RAS, Novosibirsk, Russia
[108] Department of Physics, New York University, New York NY, United States of America
[109] Ohio State University, Columbus OH, United States of America
[110] Faculty of Science, Okayama University, Okayama, Japan
[111] Homer L. Dodge Department of Physics and Astronomy, University of Oklahoma, Norman OK, United States of America
[112] Department of Physics, Oklahoma State University, Stillwater OK, United States of America
[113] Palacký University, RCPTM, Olomouc, Czech Republic
[114] Center for High Energy Physics, University of Oregon, Eugene OR, United States of America
[115] LAL, Université Paris-Sud and CNRS/IN2P3, Orsay, France
[116] Graduate School of Science, Osaka University, Osaka, Japan
[117] Department of Physics, University of Oslo, Oslo, Norway
[118] Department of Physics, Oxford University, Oxford, United Kingdom
[119] [(a)] INFN Sezione di Pavia; [(b)] Dipartimento di Fisica, Università di Pavia, Pavia, Italy
[120] Department of Physics, University of Pennsylvania, Philadelphia PA, United States of America
[121] Petersburg Nuclear Physics Institute, Gatchina, Russia
[122] [(a)] INFN Sezione di Pisa; [(b)] Dipartimento di Fisica E. Fermi, Università di Pisa, Pisa, Italy
[123] Department of Physics and Astronomy, University of Pittsburgh, Pittsburgh PA, United States of America
[124] [(a)] Laboratorio de Instrumentacao e Fisica Experimental de Particulas - LIP, Lisboa, Portugal; [(b)] Departamento de Fisica Teorica y del Cosmos and CAFPE, Universidad de Granada, Granada, Spain
[125] Institute of Physics, Academy of Sciences of the Czech Republic, Praha, Czech Republic
[126] Czech Technical University in Prague, Praha, Czech Republic
[127] Faculty of Mathematics and Physics, Charles University in Prague, Praha, Czech Republic
[128] State Research Center Institute for High Energy Physics, Protvino, Russia
[129] Particle Physics Department, Rutherford Appleton Laboratory, Didcot, United Kingdom
[130] Physics Department, University of Regina, Regina SK, Canada
[131] Ritsumeikan University, Kusatsu, Shiga, Japan
[132] [(a)] INFN Sezione di Roma I; [(b)] Dipartimento di Fisica, Università La Sapienza, Roma, Italy
[133] [(a)] INFN Sezione di Roma Tor Vergata; [(b)] Dipartimento di Fisica, Università di Roma Tor Vergata, Roma, Italy
[134] [(a)] INFN Sezione di Roma Tre; [(b)] Dipartimento di Fisica, Università Roma Tre, Roma, Italy
[135] [(a)] Faculté des Sciences Ain Chock, Réseau Universitaire de Physique des Hautes Energies - Université Hassan II, Casablanca; [(b)] Centre National de l'Energie des Sciences Techniques Nucleaires, Rabat; [(c)] Faculté des Sciences Semlalia, Université Cadi Ayyad, LPHEA-Marrakech; [(d)] Faculté des Sciences, Université Mohamed Premier and LPTPM, Oujda; [(e)] Faculté des sciences, Université Mohammed V-Agdal, Rabat, Morocco
[136] DSM/IRFU (Institut de Recherches sur les Lois Fondamentales de l'Univers), CEA Saclay (Commissariat à l'Energie Atomique et aux Energies Alternatives), Gif-sur-Yvette, France

JHEP02(2013)095

[137] Santa Cruz Institute for Particle Physics, University of California Santa Cruz, Santa Cruz CA, United States of America
[138] Department of Physics, University of Washington, Seattle WA, United States of America
[139] Department of Physics and Astronomy, University of Sheffield, Sheffield, United Kingdom
[140] Department of Physics, Shinshu University, Nagano, Japan
[141] Fachbereich Physik, Universität Siegen, Siegen, Germany
[142] Department of Physics, Simon Fraser University, Burnaby BC, Canada
[143] SLAC National Accelerator Laboratory, Stanford CA, United States of America
[144] [(a)] Faculty of Mathematics, Physics & Informatics, Comenius University, Bratislava; [(b)] Department of Subnuclear Physics, Institute of Experimental Physics of the Slovak Academy of Sciences, Kosice, Slovak Republic
[145] [(a)] Department of Physics, University of Johannesburg, Johannesburg; [(b)] School of Physics, University of the Witwatersrand, Johannesburg, South Africa
[146] [(a)] Department of Physics, Stockholm University; [(b)] The Oskar Klein Centre, Stockholm, Sweden
[147] Physics Department, Royal Institute of Technology, Stockholm, Sweden
[148] Departments of Physics & Astronomy and Chemistry, Stony Brook University, Stony Brook NY, United States of America
[149] Department of Physics and Astronomy, University of Sussex, Brighton, United Kingdom
[150] School of Physics, University of Sydney, Sydney, Australia
[151] Institute of Physics, Academia Sinica, Taipei, Taiwan
[152] Department of Physics, Technion: Israel Institute of Technology, Haifa, Israel
[153] Raymond and Beverly Sackler School of Physics and Astronomy, Tel Aviv University, Tel Aviv, Israel
[154] Department of Physics, Aristotle University of Thessaloniki, Thessaloniki, Greece
[155] International Center for Elementary Particle Physics and Department of Physics, The University of Tokyo, Tokyo, Japan
[156] Graduate School of Science and Technology, Tokyo Metropolitan University, Tokyo, Japan
[157] Department of Physics, Tokyo Institute of Technology, Tokyo, Japan
[158] Department of Physics, University of Toronto, Toronto ON, Canada
[159] [(a)] TRIUMF, Vancouver BC; [(b)] Department of Physics and Astronomy, York University, Toronto ON, Canada
[160] Faculty of Pure and Applied Sciences, University of Tsukuba, Tsukuba, Japan
[161] Department of Physics and Astronomy, Tufts University, Medford MA, United States of America
[162] Centro de Investigaciones, Universidad Antonio Narino, Bogota, Colombia
[163] Department of Physics and Astronomy, University of California Irvine, Irvine CA, United States of America
[164] [(a)] INFN Gruppo Collegato di Udine; [(b)] ICTP, Trieste; [(c)] Dipartimento di Chimica, Fisica e Ambiente, Università di Udine, Udine, Italy
[165] Department of Physics, University of Illinois, Urbana IL, United States of America
[166] Department of Physics and Astronomy, University of Uppsala, Uppsala, Sweden
[167] Instituto de Física Corpuscular (IFIC) and Departamento de Física Atómica, Molecular y Nuclear and Departamento de Ingeniería Electrónica and Instituto de Microelectrónica de Barcelona (IMB-CNM), University of Valencia and CSIC, Valencia, Spain
[168] Department of Physics, University of British Columbia, Vancouver BC, Canada
[169] Department of Physics and Astronomy, University of Victoria, Victoria BC, Canada
[170] Department of Physics, University of Warwick, Coventry, United Kingdom
[171] Waseda University, Tokyo, Japan
[172] Department of Particle Physics, The Weizmann Institute of Science, Rehovot, Israel
[173] Department of Physics, University of Wisconsin, Madison WI, United States of America
[174] Fakultät für Physik und Astronomie, Julius-Maximilians-Universität, Würzburg, Germany
[175] Fachbereich C Physik, Bergische Universität Wuppertal, Wuppertal, Germany
[176] Department of Physics, Yale University, New Haven CT, United States of America

JHEP02(2013)095

[177] Yerevan Physics Institute, Yerevan, Armenia
[178] Centre de Calcul de l'Institut National de Physique Nucléaire et de Physique des Particules (IN2P3), Villeurbanne, France

[a] Also at Department of Physics, King's College London, London, United Kingdom
[b] Also at Laboratorio de Instrumentacao e Fisica Experimental de Particulas - LIP, Lisboa, Portugal
[c] Also at Faculdade de Ciencias and CFNUL, Universidade de Lisboa, Lisboa, Portugal
[d] Also at Particle Physics Department, Rutherford Appleton Laboratory, Didcot, United Kingdom
[e] Also at Department of Physics, University of Johannesburg, Johannesburg, South Africa
[f] Also at TRIUMF, Vancouver BC, Canada
[g] Also at Department of Physics, California State University, Fresno CA, United States of America
[h] Also at Novosibirsk State University, Novosibirsk, Russia
[i] Also at Department of Physics, University of Coimbra, Coimbra, Portugal
[j] Also at Department of Physics, UASLP, San Luis Potosi, Mexico
[k] Also at Università di Napoli Parthenope, Napoli, Italy
[l] Also at Institute of Particle Physics (IPP), Canada
[m] Also at Department of Physics, Middle East Technical University, Ankara, Turkey
[n] Also at Louisiana Tech University, Ruston LA, United States of America
[o] Also at Dep Fisica and CEFITEC of Faculdade de Ciencias e Tecnologia, Universidade Nova de Lisboa, Caparica, Portugal
[p] Also at Department of Physics and Astronomy, University College London, London, United Kingdom
[q] Also at Department of Physics, University of Cape Town, Cape Town, South Africa
[r] Also at Institute of Physics, Azerbaijan Academy of Sciences, Baku, Azerbaijan
[s] Also at Institut für Experimentalphysik, Universität Hamburg, Hamburg, Germany
[t] Also at Manhattan College, New York NY, United States of America
[u] Also at CPPM, Aix-Marseille Université and CNRS/IN2P3, Marseille, France
[v] Also at School of Physics and Engineering, Sun Yat-sen University, Guanzhou, China
[w] Also at Academia Sinica Grid Computing, Institute of Physics, Academia Sinica, Taipei, Taiwan
[x] Also at School of Physics, Shandong University, Shandong, China
[y] Also at Dipartimento di Fisica, Università La Sapienza, Roma, Italy
[z] Also at DSM/IRFU (Institut de Recherches sur les Lois Fondamentales de l'Univers), CEA Saclay (Commissariat à l'Energie Atomique et aux Energies Alternatives), Gif-sur-Yvette, France
[aa] Also at Section de Physique, Université de Genève, Geneva, Switzerland
[ab] Also at Departamento de Fisica, Universidade de Minho, Braga, Portugal
[ac] Also at Department of Physics, The University of Texas at Austin, Austin TX, United States of America
[ad] Also at Department of Physics and Astronomy, University of South Carolina, Columbia SC, United States of America
[ae] Also at Institute for Particle and Nuclear Physics, Wigner Research Centre for Physics, Budapest, Hungary
[af] Also at California Institute of Technology, Pasadena CA, United States of America
[ag] Also at Institute of Physics, Jagiellonian University, Krakow, Poland
[ah] Also at LAL, Université Paris-Sud and CNRS/IN2P3, Orsay, France
[ai] Also at Faculty of Physics, M.V.Lomonosov Moscow State University, Moscow, Russia
[aj] Also at Nevis Laboratory, Columbia University, Irvington NY, United States of America
[ak] Also at Department of Physics and Astronomy, University of Sheffield, Sheffield, United Kingdom
[al] Also at Department of Physics, Oxford University, Oxford, United Kingdom
[am] Also at Department of Physics, The University of Michigan, Ann Arbor MI, United States of America
[an] Also at Discipline of Physics, University of KwaZulu-Natal, Durban, South Africa
[*] Deceased

JHEP02(2013)095